Drug and Alcohol Dependence

Convergent gray matter alterations across drugs of abuse and network-level implications: A meta-analysis of structural MRI studies

--Manuscript Draft--

Manuscript Number:	
Article Type:	Full Length Article
Section/Category:	Neuroimaging
Keywords:	gray matter; substance abuse; morphometry; hierarchical clustering; functional connectivity; meta-analytical connectivity modeling
Corresponding Author:	Matthew T Sutherland, Ph.D. Florida International University Miami, FL United States
First Author:	Lauren D Hill-Bowen, MS
Order of Authors:	Lauren D Hill-Bowen, MS
	Michael C Riedel, PhD
	Taylor Salo, MS
	Jessica S Flannery, PhD
	Ranjita Poudel, PhD
	Angela R Laird, PhD
	Matthew T Sutherland, PhD
Abstract:	Background: Neuroimaging studies often consider brain alterations linked with substance abuse within the context of individual drugs (e.g., nicotine), while neurobiological theories of addiction emphasize common brain network-level alterations across drug classes. Using emergent meta-analytic techniques, we identified common structural brain alterations across drugs and characterized the functionally-connected networks with which such structurally altered regions interact. Methods: We identified 87 studies characterizing gray matter (GM) volume differences for substance users vs. non-users. Using the anatomical likelihood estimation algorithm, we identified convergent GM reductions across drug classes. Next, we performed resting-state and meta-analytic functional connectivity analyses using each structurally altered region as a seed and computed whole-brain functional connectivity profiles as the union of both maps. We characterized an “extended network” by identifying brain areas demonstrating the highest degree of functional coupling with structurally impacted regions. Finally, hierarchical clustering was performed leveraging extended network nodes’ functional connectivity profiles to delineate subnetworks. Results: Across drug classes, we identified medial frontal/ventromedial prefrontal, and multiple regions in anterior cingulate (ACC) and insula as regions displaying convergent GM reductions among users. Overlap of these regions’ functional connectivity profiles identified ACC, inferior frontal, PCC, insula, superior temporal, and putamen as regions of an impacted extended network. Hierarchical clustering revealed 3 subnetworks closely corresponding to default mode (PCC, angular), salience (dACC, caudate), and executive control networks (dlPFC and parietal). Conclusions: These outcomes suggest that substance-related structural brain alterations likely have implications for the functioning of canonical large-scale networks and the perpetuation of substance use and neurocognitive alterations.
Suggested Reviewers:	Scott Mackey msmackey@uvm.edu
	Amy Janes ajanes@mclean.harvard.edu
	Madeleine Goodkind madeleine.goodkind@va.gov

	Aaron Boes aaron-boes@uiowa.edu
	Ahmet Ceceli ahmet.ceceli@mssm.edu

Cover Letter

FIU FLORIDA INTERNATIONAL UNIVERSITY

Neuroinformatics and Brain Connectivity Laboratory

Dr. Steve Shoptaw, March 28, 2022
Editor-in-Chief, Drug and Alcohol Dependence
RE: **New original article submission**

Dear Dr. Shoptaw:

Please find enclosed our manuscript entitled, "*Convergent gray matter alterations across drugs of abuse and network-level implications: A meta-analysis of structural MRI studies*" for publication consideration in *Drug and Alcohol Dependence* as an original article.

In this manuscript, we characterized the functional profiles of structurally altered gray matter (GM) regions consistently observed across substances of abuse employing emergent coordinate-based meta-analytic techniques. We conducted a series of meta-analyses defining common and distinct regions of reduced GM volume across five drug classes comparing. Across all drugs, we observed reduced GM in medial frontal, anterior cingulate (ACC), and insula regions among substance users. When comparing alcohol versus nicotine studies, we observed distinct alcohol-related GM reductions in inferior frontal and cingulate regions. Conversely, nicotine did not demonstrate any regions displaying greater reductions in GM volume as compared to alcohol. Subsequently, we identified an extended network, a core set of regions demonstrating the highest degree of functional coupling with multiple (common) structurally impacted regions considering task-free and task-based functional connectivity assessments. Regions comprising this extended network included frontal, temporal, ACC, PCC, insula, and putamen. We then performed separate hierarchical clustering analyses on the extended network regions' task-free and task-based functional profiles to identify subnetworks for each task state. Subnetworks closely corresponded to default mode (PCC, angular gyrus), salience (dorsal ACC, putamen), and executive control (lateral prefrontal, parietal) networks that was confirmed with functional decoding which implicated possible behavioral implications.

These findings suggest that structurally altered brain regions associated with substance use across various drug categories are robustly functionally coupled with three canonical intrinsic connectivity networks (default mode, salience, and executive control). Delineating the functional subnetworks linked with drug-related structurally altered brain regions, as done in the present manuscript via coordinate-based meta-analytic methods, provides a cost-efficient synthesis of the brain-behavior relationships linked with substances of abuse. As such, we believe this manuscript would be of interest to the extensive readership of your journal in drug, alcohol, and tobacco use and dependence.

Below is a list of potential reviewers and email contacts for your consideration:

1. Scott Mackey, University of Vermont, msmackey@uvm.edu
2. Amy Janes, McLean Hospital, Harvard Medical School, ajanes@mclean.harvard.edu
3. Madeleine Goodkind, New Mexico Veterans Affairs Healthcare System & University of New Mexico, madeleine.goodkind@va.gov
4. Aaron Boes, Carver College of Medicine, Iowa City, IA, aaron-boes@uiowa.edu
5. Ahmet Ceceli, Icahn School of Medicine at Mount Sinai, ahmet.ceceli@mssm.edu
6. Erica Grodin, University of California, Los Angeles, egrodin@psych.ucla.edu
7. Luke Chang, Dartmouth College, luke.j.chang@dartmouth.edu

This manuscript's content is original research and is not currently in submission elsewhere while under consideration at *Drug and Alcohol Dependence*. All authors have contributed substantially to this manuscript. There are no financial or other relationships associated with this study that represent a conflict of interest. Thank you for your consideration of our manuscript.

Sincerely,

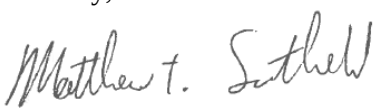

Matthew T. Sutherland, Ph.D.
Associate Professor, Departments of Psychology and Neuroscience
masuther@fiu.edu

Neuroinformatics and Brain Connectivity Laboratory (https://nbclab.github.io)
Department of Psychology • College of Arts & Sciences • Florida International University
11200 S.W. 8th Street, AHC4 Rm. 312 • Miami, FL 33199 • Tel: (305) 348-7962 • Fax: (305) 348-4289
Florida International University is an Equal Opportunity Employer and Institution - TDD via FRS 1-800-955-8771

Author Disclosures

Role of Funding Source
Nothing declared.

Contributors
Study concept and design: LDH, MCR, MTS. *Acquisition, analysis, or interpretation of data:* All authors. *Drafting of the manuscript:* LDH, MCR, MTS. *Critical revision of the manuscript for important intellectual content:* All authors. *Statistical analysis and meta-analytic tool development:* LDH, MCR, TS, ARL. *Obtained funding:* MTS, ARL. *Administrative, technical, or material support:* MTS, ARL, MCR, TS. *Study supervision:* MTS. *Data:* All data required to evaluate the conclusions in the current article are presented in the paper and/or Supplemental Materials. MTS had full access to all the data in the study and takes responsibility for the integrity of the data and accuracy of data analysis. All authors have read and approved the final manuscript.

Conflict of Interest
No conflict declared.

Acknowledgements
Primary funding for this project was provided by NIH R01 DA041353; additional support was provided by NSF 1631325, NIH U01 DA041156, NSF CNS 1532061, NIH K01 DA037819, NIH U54 MD012393.

Convergent gray matter alterations across drugs of abuse and network-level implications: A meta-analysis of structural MRI studies

Lauren D. Hill-Bowen*[,a], Michael C. Riedel*[,b], Taylor Salo[a], Jessica S. Flannery[c], Ranjita Poudel[a], Angela R. Laird[b], Matthew T. Sutherland[a†]

[a] Department of Psychology, Florida International University, 11200 SW 8th Street, Miami, FL, 33199, United States
[b] Department of Physics, Florida International University, 11200 SW 8th Street, Miami, FL, 33199, United States
[c] Department of Psychology and Neuroscience, University of North Carolina, Chapel Hill, NC

*Denotes equal first-author contributions

[†]**Correspondence:**
Matthew T. Sutherland, Ph.D.
Florida International University
Department of Psychology
AHC-4, RM 312
11200 SW 8th St
Miami, FL 33199
masuther@fiu.edu
305-348-7962

Abstract: 250 words
Text: 8,054 words
Tables: 2
Figures: 3
References: 127
Supplemental materials: 1 file

Declarations of interest: none

Highlights

- Drug use-related grey matter reductions in medial frontal, cingulate, and insula
- Extended functional impacts in inferior frontal, cingulate, insula, and putamen
- Subnetworks closely correspond to tripartite network heuristic framework
- Decoding highlights likely behavioral implications of drug-related brain changes

Abstract

Background: Neuroimaging studies often consider brain alterations linked with substance abuse within the context of individual drugs (e.g., nicotine), while neurobiological theories of addiction emphasize common brain network-level alterations across drug classes. Using emergent meta-analytic techniques, we identified common structural brain alterations across drugs and characterized the functionally-connected networks with which such structurally altered regions interact.

Methods: We identified 87 studies characterizing gray matter (GM) volume differences for substance users vs. non-users. Using the anatomical likelihood estimation algorithm, we identified convergent GM reductions across drug classes. Next, we performed resting-state and meta-analytic functional connectivity analyses using each structurally altered region as a seed and computed whole-brain functional connectivity profiles as the union of both maps. We characterized an "extended network" by identifying brain areas demonstrating the highest degree of functional coupling with structurally impacted regions. Finally, hierarchical clustering was performed leveraging extended network nodes' functional connectivity profiles to delineate subnetworks.

Results: Across drug classes, we identified medial frontal/ventromedial prefrontal, and multiple regions in anterior cingulate (ACC) and insula as regions displaying convergent GM reductions among users. Overlap of these regions' functional connectivity profiles identified ACC, inferior frontal, PCC, insula, superior temporal, and putamen as regions of an impacted extended network. Hierarchical clustering revealed 3 subnetworks closely corresponding to default mode (PCC, angular), salience (dACC, caudate), and executive control networks (dlPFC and parietal).

Conclusions: These outcomes suggest that substance-related structural brain alterations likely have implications for the functioning of canonical large-scale networks and the perpetuation of substance use and neurocognitive alterations.

Keywords: gray matter, substance abuse, morphometry, hierarchical clustering, functional connectivity, meta-analytical connectivity modeling

1. Introduction

The National Institute on Drug Abuse estimates the cost of substance use in the United States to be more than $740 billion annually (NIDA, 2017). While some treatments can improve substance use disorders and, in turn, help reduce these costs, 40-60% of patients who receive treatment for drug addiction ultimately relapse (NIDA, 2018). Drug addiction is often associated with an array of alterations in emotional, cognitive, and reward processing mechanisms which maintain drug use and make targeted treatment difficult. Despite advances in scientific research, one potential contribution to poor treatment outcomes in addiction may be due to the incomplete understanding of how drugs change the brain to foster compulsive drug use. Over the past 25 years, noninvasive brain imaging techniques, such as magnetic resonance imaging (MRI), have provided insight into the functional and structural brain alterations linked with these altered mental operations.

Brain volume studies measured by MRI are often limited by focusing on the impact of one specific substance (e.g., nicotine). As such, consensus views utilizing meta-analytic techniques also follow a similar pattern by focusing on one pharmacological class of drug. For example, meta-analyses of gray matter (GM) alterations among alcohol use disorder identified reductions in corticostriatal-limbic circuits including, the middle and anterior cingulate cortex(ACC), bilateral insulae and lenticular nuclei, extending into the left middle frontal gyrus and bilateral superior frontal gyri (Klaming et al., 2019; Xiao et al., 2015; Yang et al., 2016) that have been related to duration of alcohol use and lifetime consumption. Nicotine-related meta-analyses identified GM reductions in the ACC (Pan et al., 2012), prefrontal regions (Zhong et al., 2016), left insula, right cerebellum, parahippocampus, and thalamus for chronic users versus controls that were associated with functionally interrelated neurocircuits engaged in perception, action, and cognition

(Sutherland et al., 2016). With a smaller corpus of studies, meta-analyses of GM reductions among stimulant users versus controls have implicated the bilateral insula, right inferior frontal gyrus (Hall et al., 2015), and prefrontal cortex (Ersche, Williams, Robbins, & Bullmore, 2013). Opiate-related meta-analyses have observed GM reductions among users in fronto-temporal regions (Wollman et al., 2016). Noteworthy, reductions in GM volume, rather than increases, among individuals that use drugs (versus non-users) is often linked with clinically relevant behaviors suggesting that such alterations potentially contribute to the development and/or maintenance of substance use disorders.

In contrast to the primary literature, which historically focused on one specific substance, neurobiological theories of addiction often emphasize brain network-level impacts of substances *across* pharmacological classes of drugs (Everitt & Robbins, 2005; Goldstein, 2002; Koob & Volkow, 2010). Similarly, lesion networking mapping evaluates how the network organization of the brain may inform symptom expression associated with focal brain lesions via the lesioned site's functional connectivity patterns (Boes, 2021; Boes et al., 2015; Darby, Laganiere, Pascual-Leone, Prasad, & Fox, 2017; Kim et al., 2021; Philippi et al., 2021). Substance use disorders are often conceptualized as impacting multiple large-scale brain networks, and examining the interactions of nodes (i.e., regions) within a network, as well as between other large-scale networks may improve the characterization of addiction-related behaviors, including withdrawal (Fedota & Stein, 2015; Sutherland, McHugh, Pariyadath, & Stein, 2012b). Dysregulated activity within and between the default mode (DMN), salience (SN), and executive controls (ECN) networks has been highlighted across various neuropsychiatric disorders including addiction (Janes, Farmer, Peechatka, Frederick, & Lukas, 2015; Janes, Krantz, Nickerson, Frederick, & Lukas, 2020; Sutherland, McHugh, Pariyadath, & Stein, 2012a). These brain networks are linked with various

mental operations including: self-referential cognition, ruminations, and mind wandering (DMN; (Buckner, Andrews-Hanna, & Schacter, 2008; Greicius, Krasnow, Reiss, & Menon, 2003)), detection of and orientation to relevant internal and external events (SN; (Seeley et al., 2007)), and higher-level cognitive processes such as working memory and attentional control (ECN; (Seeley et al., 2007)). Notably, the insula, a region of the SN that orients attention to homeostatically-relevant information, has been identified as a region engaged in the dynamic switching of relative activity between the DMN and ECN (Sridharan, Levitin, & Menon, 2008b). The dynamic toggling between networks mediated by the insula may account for common cognitive alterations reported across substance use disorders including error processing (Garavan & Stout, 2005), impulsivity (Verdejo-Garcia, Lawrence, & Clark, 2008), and decision-making (Naqvi & Bechara, 2009).

The aforementioned gap between the primary literature's focus on a select drug class (with varied outcomes), and theories of common network-level alterations in addiction, potentially reflects the absence of a comprehensive classification and characterization of brain networks engaged in substance dependence regardless of substance used. One way to fill this gap is through the application of meta-analytic techniques, to gain a consensus view on structurally impacted brain regions as a function of substance use, as well as their associated functional connections throughout the brain. Furthermore, with the use of emergent coordinate-based meta-analytic techniques, we can apply a data-driven perspective to identify structurally altered regions and their associated functional networks across drug classes. A recent *image*-based mega-analysis pooled previously published data from 23 laboratories, consisting of individuals with various substance use disorders (i.e., alcohol, nicotine, cocaine, methamphetamine, cocaine) comparing subcortical volume and cortical thickness with nondependent controls (Mackey et al., 2019). In line with findings from prior meta-analytic work, results demonstrated reduced subcortical volume and

cortical thickness in substance dependent individuals, with no regions showing significantly larger volume or cortical thickness among dependent users. Regions demonstrating a shared pattern of decreased cortical thickness across drug classes included the insula, inferior parietal cortex, medial orbitofrontal cortex, middle temporal gyrus, and supramarginal gyrus (Mackey et al., 2019). A majority of the identified structurally impacted regions were found in alcohol-dependent individuals, where the amygdala and nucleus accumbens were significantly smaller among individuals who reported the highest number of drinks consumed in the past 30 days. Nicotine, methamphetamine, and cannabis failed to show any substance-specific linear effects on brain volume. Mackey and colleagues' (2019) findings are consistent with theories of addiction, where the overall pattern of volumetric effects across the brain, rather than the magnitude of a single brain region, may be important for distinguishing relevant neuroimaging biomarkers for substances dependence. Despite the utility of image-based mega-analyses for overcoming issues of low power, primary drawbacks are the cost of assembling large consortiums, managing the curation, compilation, and standardization of shared data, as well as the time it takes to aggregate data from a large number of laboratories prior to carrying out such analyses.

As such, the objective of the current study was to use *coordinate*-based meta-analytic techniques to identify and classify functional profiles of structurally altered GM regions shared across substances of abuse with data-driven behavioral decoding. We first aimed to identify consistent regions of reduced GM volume across five pharmacological classes of drugs; alcohol, nicotine, opiates, cannabis, and stimulants. Second, we aimed to delineate those brain regions with which these structurally altered areas functionally interact with, thus characterizing an extended network of impact and then further decompose this larger network into smaller subnetworks.

Finally, we aimed to delineate the putative mental operations linked with each subnetwork via meta-analytic functional decoding.

2. Methods

2.1. Analysis overview

We first conducted a literature search to compile studies reporting GM alterations among substance using individuals compared to non-using controls and applied meta-analytic techniques to identify consistent structurally altered regions across drug classes. Utilizing the regions identified in the first step, we performed resting-state and meta-analytic functional connectivity assessments to characterize the connectivity profile of each impacted region. That is, we sought to delineate what brain regions functionally interact with the ones displaying structural alterations. We then identified those brain regions showing the highest degree of functional coupling with multiple impacted regions. We termed this larger network an extended network which represents a set of regions connected to multiple structurally altered regions. To identify subnetworks within this extended network, we applied hierarchical clustering analysis leveraging the functional connectivity profiles of network nodes for both resting-state and meta-analytic assessments. Finally, to relate network-level alterations with potential behavioral implications, we employed Neurosynth functional decoding.

2.2. Identification of studies: Literature search

We performed an iterative literature search to compile peer-reviewed, MRI studies reporting structural aberrations associated with addictive disorders published up until July 2019. In the first iteration, we performed web-based searches in the *Web of Knowledge* (http://webofknowledge.com), *PubMed* (http://www.pubmed.gov), and *Google Scholar*

(http://scholar.google.com) databases, for peer-reviewed articles indexed by a combination of keywords: ("voxel-based morphometry" OR "morphometry" OR "gray matter density" OR "gray matter volume") AND ("alcohol" OR "nicotine" OR "opiates" OR "stimulants" OR "cocaine" OR "cannabis"). In the second iteration, candidate studies were identified by reviewing bibliographies of existing meta-analyses and review articles (Ersche et al., 2013; Goodkind et al., 2015; Hall et al., 2015; Klaming et al., 2019; Pan et al., 2012; Wollman et al., 2016; Xiao et al., 2015; Yang et al., 2016; Zhong et al., 2016). Finally, we examined the reference lists of relevant articles for potential studies not located during database searches or existing meta-analyses.

The inclusion/exclusion criteria for our meta-analyses were as follows. First, only empirical English language MRI studies assessing GM volume differences between substance-using individuals and healthy non-using controls were included. Second, only studies reporting whole-brain analysis outcomes of GM increases or decreases were recorded, as region of interest (ROI) analyses violate the ALE null-hypothesis that assumes equal activity across all brain regions. Third, studies reporting foci as 3D coordinates (X, Y, Z) in Talairach or Montreal Neurological Institute (MNI) stereotaxic space were included. Additional exclusion criteria included: presence of pharmacological manipulations, brain lesion studies, and participants with reports of mental and/or neurological disorders. Finally, relevant information was recorded regarding participant age and sex, substance use characteristics, MRI scanner field strength, and processing software (e.g., AFNI, FSL, SPM).

2.3. Meta-analytic procedures: Anatomical likelihood estimation

To highlight brain regions displaying convergent GM reductions across studies, we employed a revised version (S. B. Eickhoff, Laird, A. R., Grefkes, C., Wang, L. E., Zilles, K., & Fox, P. T. , 2009; Turkeltaub et al., 2012) of the anatomical likelihood estimation (ALE) algorithm

(Laird et al., 2005; Turkeltaub, Eden, Jones, & Zeffiro, 2002) as implemented in NiMARE v0.0.3, a Python package for conducting neuroimaging meta-analyses (https://nimare.readthedocs.io/en/latest/). The ALE algorithm is a voxel-based method for identifying statistically significant spatial concordance across a corpus of study coordinates by modeling brain foci as 3D Gaussian probability distributions, where the distributions' widths represent sample size variability and spatial uncertainty (S. B. Eickhoff, Bzdok, Laird, Kurth, & Fox, 2012; S. B. Eickhoff, Laird, A. R., Grefkes, C., Wang, L. E., Zilles, K., & Fox, P. T. , 2009; Laird et al., 2005). Foci reported by the primary studies as Talairach space were linearly transformed to MNI space before meta-analytic assessment (Lancaster et al., 2007). For each experimental contrast, the ALE algorithm first generated a set of modeled statistical maps, where each voxel's value corresponded to the maximum probability, and then the voxel-wise union of all modeled experimental contrasts was calculated, quantifying the spatial convergence of structural alterations throughout the brain. The resulting distribution of voxel-wise ALE values were transformed into *p*-values using a cumulative distribution function and resulting ALE maps were thresholded to highlight only voxels with $p<0.005$. Using a Monte Carlo approach, multiple comparisons correction was implemented such that a minimum cluster size threshold was determined through a set of 10,000 iterations. For each iteration, foci in the dataset were first replaced by randomly selected coordinates within a gray matter mask, ALE values were then calculated for this randomized dataset, transformed into *p*-values, thresholded at $p<0.005$, and the maximum size of supra-threshold clusters was recorded. These maximum cluster size values were used to build a null distribution, and only clusters in the original thresholded ALE map larger than the cluster size corresponding to the null distribution's 95^{th} percentile were retained in family-wise error (FEW) corrected convergence maps reported here. In other words, multiple comparisons

corrections for all analyses were applied using a cluster-forming threshold ($p_{voxel\text{-}level}$<0.005) and a cluster-extent threshold ($p_{FWE\text{-}corrected}$<0.05) (S. B. Eickhoff, Laird, Fox, Lancaster, & Fox, 2017).

Multiple ALE meta-analyses were performed identifying convergent brain regions of GM reductions across and between pharmacological classes of drugs. First, to assess convergent GM reductions *common* across all substances, a meta-analysis was performed utilizing identified coordinates from all 5 drug class studies, thus highlighting regions consistently reduced in individuals that use substances relative to non-using controls (i.e., user<control). As study reported increases (i.e., user>control) of GM volume in the literature search were limited, we did not include these coordinates in any analyses. Second, we performed separate meta-analyses for each class of drug (i.e., alcohol, nicotine, opiates, stimulants, and cannabis) to elucidate *drug-specific* regions of convergent GM reductions. Finally, to identify regions *distinctly* related with each drug, we performed pair-wise contrast meta-analyses (Laird et al., 2005) between those drugs that exhibited significant findings in individual meta-analyses of their respective studies. This contrast meta-analysis first calculated the observed difference in ALE statistics by subtracting unthresholded ALE images for each drug-specific contrast (i.e., alcohol>control – nicotine>control) from one another. Then, a null distribution of ALE difference scores was created to assess statistical significance of the observed differences. To do this, we pseudo-randomly permuted the experimental contrasts between groups, calculated voxel-level difference scores, and repeated this procedure for 10,000 iterations. Each iteration, the experimental contrasts were randomly shuffled and an equal number of contrasts to that originally observed for the drug-specific conditions were assigned to each group. Next, pseudo-ALE images were generated for these permuted groupings and subtracted from one another as before. Then, each voxel was assigned a *p*-value based on its observed difference score compared to that of the null distribution of pseudo-ALE difference

scores ($p_{FWE\text{-}corrected}$<0.05). A similar approach has been used in previous meta-analyses (Bartley et al., 2018; L. D. Hill-Bowen et al., 2021; Poudel et al., 2020). To exclude smaller regions of potential spurious differences, an additional extent-threshold of 50 continuous voxels (arbitrarily chosen) was applied. *P*-value images were then transformed to *z*-score images for visual representation.

2.4. Functional connectivity profiles of structurally altered GM regions

Following ALE meta-analyses, we extracted ROIs from the resulting significant clusters across all substances. Given that some of the clusters spanned multiple anatomical regions, which may represent distinct functional nodes, we defined ROIs by generating 6mm radius spherical seeds at the local maxima within each cluster. For this, we utilized FSL's *cluster* command and required that local maxima be distanced no less than 15-mm from each other. We then evaluated both task-free and task-based functional connectivity assessments for each ROI to identify brain regions functionally linked to drug-related structural alterations. Subsequently, we examined the conjunction of these two connectivity maps to generate a connectivity profile for each ROI that was consistent across both brain states.

2.4.1. Task-free functional connectivity: Resting-state fMRI (rs-fMRI)

Resting-state connectivity analyses typically identify those voxels of the brain that demonstrate the highest temporal correlation with the average time-course of a seed ROI and provide context about the brain's underlying functional architecture. In order to derive robust resting-state functional connectivity (rsFC) maps for each ROI, we utilized the minimally pre-processed and denoised rs-fMRI data provided by the Human Connectome Project's (HCP; (Van Essen et al., 2013)) Young Adult Study (S1200 Data Release; March 1, 2017). On November 12, 2019, 150 randomly selected participants (mean±SD: 28.7±3.9 years old) were downloaded via

the HCP's Amazon Web Services Simple Storage Solution repository. The sample included 77 females (30.3±3.5 years old) and 73 males (27.1±3.7 years old). While this age difference between biological sex was significant (t[149] = -5.3, p<0.001), it is also consistent with that noted in the full S1200 Data Release (Van Essen et al., 2013).

Detailed acquisition and scanning parameters for HCP data can be found in consortium manuscripts (Smith et al., 2013; Ugurbil et al., 2013; Van Essen et al., 2012), but relevant scan parameters are briefly summarized here. Each participant underwent T1-weighted and T2-weighted structural acquisitions and four rs-fMRI (15 minutes each) acquisitions. Structural images were collected at 0.7-mm isotropic resolution. Whole-brain EPI acquisitions were acquired on a 3T Siemens Connectome MRI scanner: 32-channel head coil, TR=720ms, TE=33.1ms, in-plane FOV=208×180 mm, 72 slices, 2.0mm isotropic voxels, and multiband acceleration factor of 8 (Feinberg et al., 2010).

The S1200 data release contains minimally pre-processed and denoised MRI data. The minimal pre-processing workflow is described in Glasser and colleagues, 2016 (Glasser et al., 2016), but consists of typical imaging pre-processing techniques that leverage the high-resolution data acquired by the HCP. First, T1- and T2-weighted images were aligned, bias field corrected, and registered to MNI space. Second, the fMRI pipeline removed spatial distortions, realigned volumes to compensate for subject motion, registered the fMRI data to structural volumes (in MNI space), reduced the bias field, normalized each functional acquisition to its corresponding global mean, and masked non-brain tissue. We note that care was taken to minimize smoothing induced by interpolation and that no overt volume smoothing was performed. The minimize physiological and/or movement artifacts, HCP functional data was automatically denoised using FMRIB's ICA-based X-noiseifier (FIX; (Salimi-Khorshidi et al., 2014)) to auto-classify independent components

analysis (ICA) components as either "signal" (i.e., brain activity) or "noise" (e.g., non-neuronal signals) using multiple spatial and temporal features via pattern classification. Briefly, ICA was performed on each functional dataset independently and characteristics of each component, such as spatial localization and power in high-frequencies, were evaluated by a classifier to determine if a given component is related to neuronal activity or artifact. The time-series corresponding to artifactual components are then regressed out of the data, providing a "cleaned", denoised dataset for further investigation.

Using the minimally pre-processed, denoised resting-state datasets for each participant, the average time course for each ROI was extracted, as well as the average time course across all brain voxels. In independent deconvolutions for each ROI, the "global signal" was entered as a regressor of no interest using FSL's FEAT tool (Jenkinson, Beckmann, Behrens, Woolrich, & Smith, 2012), which also incorporated spatial smoothing with a FWHM of 6mm. The "global signal", although controversial, was included in the regression under the assertion that it performed better than other commonly used motion-correction strategies in removing motion-related artifacts in the HCP rs-fMRI data (Burgess et al., 2016). The results from multiple runs (4, 15 minute) within a participant for each ROI were then averaged using a fixed-effects analysis. A group-level, mixed-effects analysis (Woolrich et al., 2009) was then performed to derive a rsFC map for each ROI. Images were thresholded non-parametrically using Gaussian Random Field theory-based maximum height thresholding with a (voxel FWE-corrected) significance threshold of $p<0.001$ (Worsley, 2001), such that more spatially specific connectivity maps could be derived when using such a highly powered study (Woo, Krishnan, & Wager, 2014).

2.4.2. Task-based functional connectivity: Meta-analytic co-activation modeling (MACM)

Using reported coordinates from task-based fMRI studies, meta-analytic co-activation identifies locations in the brain that are most likely to be co-activated with a given seed ROI across multiple task-states (Laird et al., 2009). Thus, differing from rsFC, MACM provides context about neural recruitment during task-based behaviors. We therefore aimed to integrate these two complementary modalities by supplementing the rsFC maps with MACM maps for each ROI. To do so, we relied on the Neurosynth (Yarkoni, Poldrack, Nichols, Van Essen, & Wager, 2011) database, which contains the published stereotactic coordinates from over 14,000 fMRI studies and 150,000 brain locations. Neurosynth relies on an automated coordinate extraction tool to "scrape" (i.e., compile) each available fMRI study for all reported coordinates. Given this automated nature, fMRI studies that report the results of multiple experimental contrasts as separate sets of coordinates are amalgamated into one set of coordinates, and "activation" or "de-activation" coordinates are not distinctly characterized. While this inherent noise may yield greater limitations in interpretation, the power over manually curated datasets outweighs the potential confounds of bi-directional or mixed-contrast effects.

To generate a MACM map for each ROI, we utilized NiMARE to search the Neurosynth database for all studies reporting a coordinate within the defined ROI mask. Neurosynth tools support the multilevel kernel density analysis (MKDA) algorithm for performing meta-analyses. However, we opted to use the ALE algorithm (as implemented in NiMARE) given its optimal performance in replicating image-based meta- and mega-analyses (Salimi-Khorshidi, Smith, Keltner, Wager, & Nichols, 2009). While the standard ALE algorithm requires participant sample sizes to generate a smoothing kernel for blurring the coordinates, the Neurosynth database does not. As such, we employed a 15mm FWHM smoothing kernel for all study coordinates, as this parameters value has shown the greatest correspondence with "gold standard" image-based meta-

analysis outcomes (Salimi-Khorshidi et al., 2009). Once ALE maps were generated for each ROI, voxel-FWE correction (p<0.001) was performed to parallel rsFC map thresholding.

2.4.3. Consensus across rs-fMRI and MACM connectivity assessments

rsFC and MACM provided two independent, but complementary, modalities during task-free and task-based states, respectively, for demonstrating connectivity between each ROI and the rest of the brain. In our exploration to identify brain regions functionally connected to structurally altered brain regions, we wanted to utilize robust connectivity profiles that characterized connectivity across both task states. Thus, we obtained a consensus map using FSL tools for each ROI by creating a binary mask that only included those voxels that were significant in each ROI's respective rsFC and MACM maps.

2.5. Delineation of an extended network and associated functional cliques

To derive a set of core regions functionally coupled to multiple structurally impacted regions, we first summed all the binarized consensus maps that were calculated by evaluating the conjunction of each ROI's respective rsFC and MACM maps. We then only considered those regions in which at least 3 ROIs demonstrated significant connectivity across modalities. We opted for a minimum overlap of 3 because it indicates the existence of a network guaranteed to include membership from more than just two regions highly co-activating with each other (Camilleri et al., 2018). After thresholding the summed map, and only considering those clusters with a minimum extent of at least 10 voxels, we then identified coordinates as local peaks separated by a distance of at least 15mm. The identified core regions represent a larger functional network of impact we termed an "extended network", similar to other previous applications (Amft et al., 2015; Camilleri et al., 2018). Following the identification of regions comprising the extended network, we examined the organization of these regions into functional cliques. To do so, we first calculated

rsFC and MACM connectivity assessments for each ROI. We then entered the corresponding connectivity maps, separately for each modality, into a hierarchical clustering analysis to yield functional cliques of input regions.

2.5.1. rs-fMRI and MACM functional connectivity

Spherical ROIs with a radius of 6mm were generated around the regions of the extended network. Following the same procedures described above, a rsFC map was calculated utilizing HCP rs-fMRI data for each ROI, and a MACM map was calculated in NiMARE for each ROI using the ALE algorithm, which identified consistent brain locations reported across studies from the Neurosynth database that reported a coordinate in the respective ROI.

2.5.2. Identifying cliques through hierarchical clustering

We next sought to identify functional cliques within the extended network by performing hierarchical clustering analyses to subgroup ROI seeds with similar functional connectivity profiles based on their: 1) resting-state functional connectivity patterns (i.e., task-free), and 2) meta-analytic coactivation patterns (task-based). In MATLAB (v2013b; Natick, MA), unthresholded rsFC and MACM maps were imported using Statistical Parametric Mapping (SPM; Wellcome Trust Centre for Neuroimaging, London) tools, and three-dimensional images were vectorized and concatenated to create a VxM matrix, where V was the number of voxels in the standard MNI152 2mm resolution brain template and M was the number of maps. Then, an agglomerative hierarchical cluster tree was calculated for rsFC, and separately MACM, which described how the input ROIs clustered together based on the similarity of their respective functional connectivity maps. This approach yielded a data-driven characterization of regions that demonstrate similar functional profiles.

To provide a rudimentary example of how hierarchical clustering works, the maps for two ROIs found to be the most similar constitute a cluster. Then, the map for a third ROI is considered and may be found to be very similar to the previous two; in this instance, another branch is added to the tree to include the third ROI. However, if the map for a third ROI is more similar to a fourth map, then those two constitute a cluster, and an additional branch is added to merge the cluster from the former two ROIs and the latter two ROIs. Two methods that require special attention when building the tree are how similarity between variables is determined ('distance') and how the distance between clusters is calculated ('linkage'). First, similarity between variables is calculated as the distance between variables. The distance can be calculated using a number of algorithms, which Euclidean distance or correlation to provide the most commonly used. Second, methods for calculating the distance between clusters include using the average, largest, or smallest distance between each of its respective variables (*average, complete*, *single,* respectively). More complex algorithms use the inner-squared distance of the cluster centers, such that clustering solutions are determined by minimizing the within-cluster variance after merging variables (*Ward's minimum variance algorithm*). Given the complexity in describing the results of agglomerative hierarchical cluster trees, dendrograms are commonly used to visualize the results of hierarchical clustering analysis. A dendrogram represents all variables entered into the clustering analysis on one axis and distance on the second axis. Variables are joined together as clusters using branches, and the distance between two variables or clusters is indicated by the branch height on the distance axis.

We utilized the *Euclidean* 'distance' method and *Ward's minimum variance* 'linkage' algorithm to calculate the agglomerative hierarchical cluster tree for unthresholded rsFC and MACM maps, separately. We used unthresholded maps to reduce the effects of sparsity when

using thresholded maps. It is possible (and likely) for hierarchical clustering outcomes to differ (i.e., seeds assigned to different cliques or differing number of cliques) using task-free and task-based fMRI data. We then visualized our results using a dendrogram and selected the most theoretically interesting and feasible clustering solution for describing functional cliques impacted by drug-related structural alterations.

2.6. Behavioral inferences of task-based functional cliques

Hierarchical clustering analyses performed in the previous step yielded distinct cliques of regions that demonstrated similar whole-brain connectivity profiles. We then leveraged the average, unthresholded MACM map across regions within a clique to perform functional decoding analyses in Neurosynth, thus providing insight into the mental operations putatively linked with each clique/cluster/subgroup.

The Neurosynth database automatically curates using two pieces of information from >14,000 fMRI studies: article abstract text and reported coordinates. In short, terms from article abstract text are vectorized based on their frequency of occurrence within and across all studies, a metric known as the term frequency-inverse document frequency. Only ~1,300 terms with the highest frequencies are retained for meta-analytic purposes. If a given fMRI study contains a term with a frequency above a given threshold (0.001), then that study will have been automatically annotated with that term. Coordinates from each study are automatically extracted from the text and a binary spherical ROI with a radius of 10mm is generated around each coordinate. A meta-analytic map for each term is then generated by identifying those studies that were annotated with the given term and then performing a MKDA, which assesses the activation frequency for a given voxel in studies that were annotated with the respective term compared to studies that were not annotated with the term. Note that this is a different meta-analytic algorithm than the ALE

algorithm described above. Functional decoding may then be performed by a simple correlation between a user-provided map and the meta-analytic map derived for each term.

We performed functional decoding analyses on each functional clique by first calculating the average MACM map using each clique's respective ROI MACMs, and then correlating the averaged map with every term's map in Neurosynth. Currently, there is no established statistical test for determining whether a term is "significantly" associated with a given map; however previous approaches (Bottenhorn et al., 2019; Flannery et al., 2020; L. D. Hill-Bowen, Riedel, M.C., Poudel, R., Salo, T., Flannery J.S., Camilleri, J.A., Eickhoff, S.B., Laird, A.R., Sutherland, M.T., 2020) have interpreted the top functional and anatomical terms, while disregarding terms that provide less interpretational value. For example, prior work has classified Neurosynth terms as 'functional', 'anatomical', 'non-content', or 'participant-related' (https://github.com/62442katieb/ns-v-bm-decoding). Here, we identified the top 10 anatomical and 10 functional terms displaying the highest correlations with each clique's input map. Any term that designated a duplicate (or synonym) of one already identified was recorded, but not included in the list (see **Supplemental Table S2** for details).

3. Results

3.1. Literature search outcomes

Following the outlined inclusion/exclusion criteria, we located a total of 84 peer-reviewed articles composed of 87 experiments/contrasts involving a total of 654 brain foci reporting GM reductions in substance users (3,533 participants) compared to non-users (3,405 participants) across five drug classes (**Supplemental Table S1**). These articles included 21 alcohol (22 experiments, 213 foci), 17 nicotine (18 experiments, 95 foci), 25 stimulant (26 experiments, 239

foci), 9 cannabis (9 experiments, 37 foci), and 12 opiate studies (12 experiments, 70 foci). A PRISMA flow diagram depicting the literature search and article inclusion process is provided in **Supplemental Figure S1**. Substance-using participants from included articles were 35.13±9.88 (mean ± SD) years old and consisted of 1,031 females and 2,489 males with an on average greater proportion of males than females, $t(84)=1.98$, $p<0.001$. Non-using participants from included articles were 34.26±9.91 years old and consisted of 1,208 females and 2,194 males with on average a greater proportion of males than females, $t(82)=1.98$, $p<0.05$.

3.2. Convergent GM reductions across and within drugs: Meta-analytic outcomes

To first identify regions consistently demonstrating reduced GM volume across the five drug classes, we conducted a meta-analysis of all identified studies for the contrast user versus non-using control (i.e., user<control). Convergent GM reductions were observed notably in seven regions, right anterior and middle cingulate, bilateral medial frontal, left superior frontal, and multiple regions within the left insula (**Fig. 1A; Table 1A**). To characterize drug specificity, we conducted a series of separate meta-analyses for each drug class. When considering only alcohol articles, significant convergent GM reductions were identified in the bilateral cingulate, left inferior frontal, and left postcentral regions **(Fig. 1B; Table 1B)**. When considering only nicotine articles, significant convergent GM reductions were identified in multiple regions within the posterior cingulate cortex (PCC) **(Fig. 1C; Table 1C)**. Drug-specific meta-analyses for cannabis, opiates, and stimulants failed to yield significant clusters. Cannabis-related and opiate-related null results may be attributed to a lack of sufficient published experimental contrasts in the literature (best practices recommends approximately 20 contrasts) (S. B. Eickhoff et al., 2016). To further delineate distinct patterns of reduced GM volume between drug classes, we conducted two contrast analyses, excluding those with null drug-specific convergence (i.e., cannabis, opiates, stimulants).

When considering direct statistical comparisons between drug categories, alcohol (vs. nicotine) was linked with greater convergent reductions in the left inferior frontal, and bilateral cingulate gyrus (i.e., alcohol>nicotine) **(Fig. 1D; Table 1D)**; whereas, nicotine did not result in any significant clusters demonstrating greater reductions in GM as compared to alcohol (i.e., nicotine>alcohol).

3.3. Task-based and task-free connectivity of structurally altered regions

To identify brain regions functionally connected to structurally altered regions, we generated rsFC and MACM maps independently for the resulting significant clusters in the meta-analysis across all drug classes (**Supplemental Fig. S2, rsFC & MACM**). Further, to provide consensus views across both brain states within a seed region, voxels that were significant in both the resting-state and meta-analytic thresholded connectivity maps were retained to yield a consensus map that was a modality-agnostic representation of connectivity (**Supplemental Fig. S2, consensus**).

3.4. Extended network regions and hierarchical clustering

To derive a core set of regions demonstrating the highest degree of functional coupling with multiple structurally impacted regions, we summed all ROI modality-agnostic (i.e., consensus) maps. Core regions comprising the extended network included multiple regions within the right anterior cingulate (ACC) and left inferior frontal, bilateral PCC, right insula, right superior temporal, and left putamen (**Fig. 2A; Table 2**).

To further examine the organization of extended network regions into functional cliques, we calculated rsFC and MACM maps for each of these ROIs (**Supplemental Fig. S3**). The resulting seed-based functional connectivity maps were then entered into the hierarchical clustering algorithm, providing a clustering solution for each task state (i.e., rsFC and MACM

maps), separately. Both rsFC and MACM clustering solutions revealed three primarily consistent cliques, with a few notable differences (**Fig. 2B-C**). Clique 1 was largely consistent across both solutions, demonstrating similar activation profiles for the PCC and right superior temporal lobe. Clique 1 was additionally linked with co-activation in medial frontal regions, bilateral parietal lobules, and bilateral temporal gyrus (**Fig. 2, red**). The two solutions differ in that the ACC clusters with the PCC and superior temporal lobe in the task-based solution (i.e., MACM), but not in the task-free solution (i.e., rsFC). Clique 2 was consistent across solutions in demonstrating similar activation profiles for the left putamen and left inferior frontal gyrus. Clique 2 was additionally associated with co-activation in the cingulate gyrus and right inferior frontal (sparser in the rsFC solution) (**Fig. 2, green**). A notable difference between the solutions is in the inclusion of the ACC seed region, MACM Clique 2 includes a more caudal ACC seed region, while rsFC Clique 2 incudes a more rostral ACC seed region. Clique 3 demonstrated consistency across both solutions in clustering of the left inferior frontal, right cingulate, and right insula. Clique 3 was additionally linked with co-activation in bilateral parietal regions, and in the MACM solution additionally the bilateral middle frontal gyri (**Fig. 2, blue**). The two solutions differ in that the ACC clusters in the inferior frontal gyrus, cingulate, and insula in the task-free solution, but not in the task-based solution.

3.5. Functional decoding of task-based cliques

We performed functional decoding on each task-based clique to garner insight into associated psychological processes. The top 10 unique Neurosynth functional and anatomical terms with the highest correlation values for each clique were taken into consideration (**Fig, 3; Supplemental Table S2**). Neurosynth decoding outcomes were used to guide the following functional interpretation of each clique:

Clique 1 (**Fig. 3B, red**) was composed of superior temporal, PCC and ACC regions, reminiscent of the canonical default mode network, which were associated with the Neurosynth functional terms: *retrieval, engaged, memory retrieval, general, mentalizing, autobiographical, theory, mind, default*, and *mental*. These functional decoding outcomes suggest this clique was associated with memory and self-referential processes.

Clique 2 (**Fig. 3B**, **green**) consisted of putamen, inferior frontal, and ACC, reminiscent of the canonical salience network, which were associated with the Neurosynth functional terms: *reward, incentive, monetary, anticipation, motivation, response, general, incentive delay*, *task,* and *errors*. These decoding outcomes suggest this clique was linked with the occurrence of motivationally important (i.e., salient) events.

Clique 3 (**Fig. 3B**, **blue**) included the inferior frontal, insula, and cingulate, reminiscent of the canonical executive control network, which were associated with the Neurosynth functional terms: *task, demands*, *general*, *conflict*, *working memory*, *task difficulty*, *response inhibition*, *stimulus*, *load*, and *word*. These outcomes suggest this clique was related to executive and attentional functions.

4. Discussion

Here, we identified and classified the functional profiles of structurally altered GM regions across five pharmacological classes of drugs employing emergent meta-analytic techniques. We first demonstrated that across substances of abuse (i.e., alcohol, nicotine, opiates, cannabis, and/or stimulants), substance users demonstrated decreased GM volume in medial frontal, ACC, and insula regions as compared to non-users. Alcohol-specific reductions were apparent in the dACC, inferior frontal, and postcentral regions, while nicotine-specific reductions were apparent in the PCC. Second, we delineated those brain regions with which these structurally altered regions across drugs functionally interact with utilizing task-free and task-based functional connectivity assessments, thus characterizing an extended network of impact. This extended network included regions of the anterior and posterior cingulate, inferior frontal, insula, superior temporal, and putamen regions. Finally, we decomposed this larger extended network into smaller subnetworks and subsequently linked each subnetwork with more elemental mental operations. Based on these brain and behavioral profiles, we suggest that structurally altered brain regions associated with

substance use across various drug categories are robustly functionally coupled with three large-scale brain networks associated with memory and self-referential processes, motivationally important (i.e., salient) events, and executive and attentional functions.

4.1. Structural alterations across and within drug classes

Reductions in GM volume for substance users compared to non-users were present across drug classes, as well as within specific substances (i.e., alcohol, nicotine). Across various substances, brain regions displaying reduced GM volume included the superior and medial frontal gyrus, and multiple regions in the ACC and insula that is supported by previous evidence. Of particular interest, Mackey and colleagues (2019) *image*-based mega-analytic results identified the insula, parietal cortex, and medial orbitofrontal regions for substance in general that have been frequently linked to substance dependence and potentially predict increased craving and relapse risk (Mackey et al., 2019; Seo et al., 2013; Sutherland et al., 2015). Our results replicate these findings in the insula and medial orbitofrontal/ventromedial prefrontal cortex (vmPFC), while extending new findings to the ACC. The insula is thought to be critically engaged in the perception of the internal bodily state, with more posterior regions involved in homeostatic motor functions, and more anterior regions involved in motivation (Craig, 2009). Damage involving the insula, compared to damage of regions not including the insula, has shown to disrupt smoking addiction, more specifically quit smoking easily, immediately, without relapse, and without persistent craving in cigarette smokers (Naqvi, Rudrauf, Damasio, & Bechara, 2007). Current treatment approaches have demonstrated promise of the insula as a target for brain stimulation techniques such as transcranial magnetic stimulation, transcranial direct current stimulation, and deep brain stimulation in substance use disorders (Ibrahim et al., 2019). The medial frontal region, or vmPFC, is thought to be engaged during goal-directed action selection, such as when learning new

stimulus-reward contingencies, or when environmental demands are changing (Ridderinkhof, van den Wildenberg, Segalowitz, & Carter, 2004). The Iowa Gambling Task (IGT) incorporates elements of reward, risk, punishment, uncertainty, and changing contingencies, that was developed to test the performance of patients with vmPFC damage (Bechara, Damasio, Damasio, & Anderson, 1994). Throughout the task, neurologically healthy individuals avoid bad decks (associated with net loss of money), while selecting good decks (associated with net gain of money) more frequently, while also demonstrating changes in skin conductance response before selecting from bad decks. In contrast, patients with vmPFC damage continue to select from bad decks, with no anticipatory skin conductance response (Bechara, Damasio, Tranel, & Damasio, 1997). Together, this suggests that disruption of the vmPFC may impact the individual's ability to accurately compute stimulus value and make advantageous value-based decisions (Schneider & Koenigs, 2017). The ACC, more specifically the dorsal ACC (dACC), is engaged in cognitive control carrying value-related information essential for regulating behavioral persistence and flexibility (as during reward-based decision-making) (Kolling et al., 2016; Shenhav, Cohen, & Botvinick, 2016). Lesioning dACC has shown variable degree of impairment in cognitive processes involving error correction (Hochman, Wang, Milner, & Fellows, 2015; Shima & Tanji, 1998), using rewards to guide choice behavior (Kennerley, Walton, Behrens, Buckley, & Rushworth, 2006; Rushworth, Walton, Kennerley, & Bannerman, 2004), and decision-making assessing relative values of behavior persistence versus change (Buckley, Mansouri, & Tanaka, 2009; Camille, Tsuchida, & Fellows, 2011). Collectively, the present results suggest a shared set of neural alterations that are robust across drug classes in regions associated with motivation, goal-directed behaviors, and allocation of control.

Alcohol-specific reductions in GM volume were apparent in the dACC, inferior frontal, and postcentral gyrus. Mackey and colleagues (2019) found alcohol-specific effects to be widespread throughout the brain (27 ROIs), yet failed to find any other drug-specific effects in nicotine, methamphetamine, or cannabis. Our results replicate alcohol-specific findings in the precentral and caudal middle frontal gyri (as extensions of the inferior frontal cluster, see Fig. 1B), while extending new findings to more dorsal regions of the ACC (as they report more rostral ACC), inferior frontal, and postcentral gyrus. The inferior frontal gyrus (Brodmann's area 9), or dorsolateral prefrontal cortex (dlPFC), is critically engaged in cognitive control (i.e., executive functions), including decision making, response inhibition, risk-taking, and attentional bias. Brain stimulation studies focusing on drug addictions have targeted the dlPFC as the primary target for its engagement in cue-elicited craving and cognitive alterations commonly associated with addictions (e.g., impulsivity) (Alizadehgoradel et al., 2020; Su et al., 2017). During a probabilistic visual discrimination reversal test (O'Doherty, Kringelbach, Rolls, Hornak, & Andrews, 2001), individuals with dlPFC lesions failed to pay attention to critical feedback presented on the screen following each trial regarding the amount won or lost that resulted in task performance impairments (Hornak et al., 2004). In contrast to individuals with orbital prefrontal lesions showing deficits in monitoring changes in the reward value of a stimulus, and using this to guide behavior, individuals with dlPFC lesions show deficits related to executive functions, such as the control of attention (Hornak et al., 2004).

Nicotine-specific reductions in GM volume converged in the PCC. Supported by prior work, the PCC is suggested to maintain balance between internal and external directed thought (Binder et al., 1999; Leech, Kamourieh, Beckmann, & Sharp, 2011), attribution of personal meaning to salient events (Andrews-Hanna, Smallwood, & Spreng, 2014), and engaged in

subjective evaluative processes in reward-guided decision making (Hayden, Nair, McCoy, & Platt, 2008; Pearson, Heilbronner, Barack, Hayden, & Platt, 2011). Individuals with lesions to this region present with deficits in the regulation of attentional focus (Kumral, Erdogan, Bayam, & Arslan, 2019), and those with stroke damage have been shown to result in the complete disruption of cigarette smoking (Jarraya et al., 2010). We and others have proposed that the functional interactions between the PCC and other regions of the DMN potentially contribute to ruminations about substance use, perpetuating the addiction cycle (L. D. Hill-Bowen et al., 2021; Sutherland et al., 2012a; Sutherland & Stein, 2018; Zhang & Volkow, 2019). As such, the PCC has emerged as a key target region for interventions mitigating craving and in turn, drug use (Janes et al., 2019).

Contrast meta-analytic outcomes distinct to alcohol (i.e., alcohol > nicotine) identified the dACC and inferior frontal gyrus/dlPFC. As aforementioned, both the dACC and dlPFC are critically engaged in cognitive control mechanisms and maintain strong reciprocal interconnections (Bush, Luu, & Posner, 2000; Devinsky, Morrell, & Vogt, 1995; Koski & Paus, 2000). Computational models of conflict-driven feedback, as a mechanism by which the brain adjusts cognitive control, suggest the ACC detects instances of conflict (conflict-monitoring role) and relays signals to other regions, such as the dlPFC to implement cognitive control and adjust performance (Botvinick, Braver, Barch, Carter, & Cohen, 2001; Mansouri, Tanaka, & Buckley, 2009). It is notable that these regions were distinct to alcohol, as brain stimulation treatments for addictions, across drug categories and psychiatric disorders, have stimulated the dlPFC (Salling & Martinez, 2016). These results being distinct to alcohol only may potentially reflect the lack of consistency in the literature from low effect sizes and insufficient power to detect true effects in other categories of drugs (Mackey et al., 2019).

4.2. The extended network and associated subnetworks

Pharmacological classes of drugs are often conceptualized as having effects on numerous brain circuits and networks, rather than a specific lesion or activation in circumscribed brain regions (Koob & Volkow, 2010, 2016; Volkow, Michaelides, & Baler, 2019). Lesion network mapping incorporates network effects into neurological symptom localization, as often symptoms fail to localize to a single brain region, or arise from dysfunction in connected regions to the lesion site, rather than the site itself (Boes et al., 2015; Ferguson et al., 2019; Joutsa, Shih, & Fox, 2019; Padmanabhan et al., 2019). As such, we examined the functional connectivity profiles, both task-free and task-based, of convergent GM reductions across substances to elucidate additional regions concurrently engaged. We then identified those regions demonstrating the highest degree of functional coupling with multiple structurally impacted regions, we termed this larger network an extended network. Working under the assumption that this larger extended network can be decomposed into smaller subnetworks, we employed a principled clustering approach leveraging the functional connectivity maps (task-free and task-based) of ROI seed regions. This identified three distinct subnetworks, for which we then employed Neurosynth functional decoding to characterize the putative mental operations linked with each subnetwork. The three identified subnetworks closely correspond to the tripartite network parcellation, where the dynamic interactions between and within these large-scale brain networks has shown to have important implications in addictions.

4.2.1. Spiraling fronto-striatal circuits

Identified subnetworks for task-based and task-free functional connectivity revealed largely similar groupings of ROI seed regions, where subnetwork 1 in red demonstrated a functional connectivity profile with the PCC, subgenual ACC, medial frontal, parietal, and temporal regions. Subnetwork 2 in green, demonstrated a connectivity profile consisting of the

putamen, inferior frontal, and dACC. Subnetwork 3's profile in blue included inferior and middle frontal gyri, insula, cingulate, and parietal regions. This apparent shift from ventral ACC to dorsal ACC to posterior, supplementary motor area seen in the transition from subnetwork 1 to subnetwork 3 potentially is consistent with a hierarchy of information flow seen in spiraling fronto-striatal circuits (Haber, Fudge, & McFarland, 2000). Information from the limbic system does not reach the motor system through direct connections, but rather through a series of ascending circuits. The ventromedial striatum contains two subdivisions, the "shell" distinguished by its limited input from the cortex, midbrain, and thalamus, and the "core" (Zaborszky et al., 1985; Zahm & Brog, 1992). The core subdivision receives input from the orbital and medial prefrontal cortex, while the shell receives forebrain input from the amygdala, hippocampus, and limited regions of the medial cortex. The dlPFC projects to the central striatum, and premotor and motor cortex projects to the dorsolateral striatum. The midbrain projections from the shell form a reciprocal loop with both the ventral tegmental area and ventromedial substantia nigra, pars compacta, where projections from more medial areas feedforward to the core. This spiral advances through striatonigrostriatal (SNS) projections from the core that then project more dorsally. Through this process, ventral striatal regions influence more dorsal striatal regions through spiraling SNS projections. Together, this hierarchy of information flow seen in spiraling fronto-striatal circuits is commonly engaged in reward processing and goal-directed behaviors that require motivations to drive behavior, cognition that organizes and plans the strategy, and ultimately the execution of those motor plans (Haber, 2003; Haber et al., 2000; Pauli, O'Reilly, Yarkoni, & Wager, 2016).

4.2.2. Tripartite network integration

Consistent with the aforementioned series of ascending circuits, through data-driven meta-analytic techniques, we identified three subnetworks (task-based) with meta-analytic decoding results suggesting functional characterization of value-based decision making, emotional and reward saliency, and attentionally driven cognitive functions that correspond to the tripartite network heuristic framework. The tripartite network parcellation consists of three large-scale brain networks (Menon, 2011). The DMN, centered around nodes in the medial prefrontal cortex, medial temporal lobe, angular gyrus, and PCC, is typically deactivated during stimulus-driven cognitive tasks (Greicius et al., 2003) and implicated in value-based decision making (Rangel, Camerer, & Montague, 2008), self-referential processes (Qin & Northoff, 2011), and memory (e.g., episodic memory retrieval and autobiographical) (Sestieri, Corbetta, Romani, & Shulman, 2011; Spreng, Mar, & Kim, 2009). The SN, anchored in the dACC and fronto-insular cortex, has been linked with orienting attention to internal or external stimuli (Seeley et al., 2007; Sridharan, Levitin, & Menon, 2008a), and affective processes (Menon & Uddin, 2010). The ECN, a frontoparietal system with primary nodes in the dlPFC and lateral posterior parietal cortex, has been engaged in processing exogenous, attentionally driven cognitive functions such as goal-directed behavior (Fox et al., 2005; Honey, Kotter, Breakspear, & Sporns, 2007; Petrides, 2005). The dynamic connectivity within and between these three large-scale brain networks has important implications in examining the neurocognitive alterations associated with psychopathology and addictions (Sha, Wager, Mechelli, & He, 2019; Sutherland et al., 2012b).

The brain processes environmental stimuli in a continuous flow, where information from both exogenous and endogenous sources is integrated to control mechanisms that orient, identify, and act upon the most salient stimuli. This coordination between exogenous and endogenous information is often critically impaired in most psychiatric disorders (Menon, 2011; Sha et al.,

2019; Uddin, 2015) and addictions (Sutherland et al., 2012b) that is primarily modulated by the SN "toggling" between internally directed attention subserved by the DMN, and externally directed executive functions subserved by the ECN. In psychiatric disorders, the SN demonstrates hypoconnectivity with the DMN and ECN that is involved in goal-directed regulation and self-referential processing respectively, while dorsal SN exhibits hyperconnectivity between the DMN, as well as between the DMN and ECN. This combination of both hypo- and hyper- connectivity can be ascribed to distinct parts of the insula exhibiting distinct patterns of functional connectivity (Chang, Yarkoni, Khaw, & Sanfey, 2013; Deen, Pitskel, & Pelphrey, 2011; Taylor, Seminowicz, & Davis, 2009). In addictions, during stages of withdrawal, increased engagement of the insula during abstinence has shown to augment normative network switching between the DMN and ECN that potentially explains the reduction in negative coupling, where typically increased activation in ECN corresponds to increased deactivation of DMN (Fox et al., 2005; Sutherland et al., 2012b). Further, chronic smokers as compared to non-smokers have exhibited reduced connectivity within DMN key hubs including the medial prefrontal and PCC nodes, as well as within ECN key hubs including the dlPFC and parietal nodes that was correlated with duration and frequency of chronic use (Weiland, Sabbineni, Calhoun, Welsh, & Hutchison, 2015). As such, a systems-level perspective of the neurocognitive mechanisms underlying substance dependence could potentially inform biomarkers for disease severity and symptomatology.

4.3. Limitations

Several potential limitations warrant attention. First, characterization of the substance-using group across included studies is not uniform within our sample, as reported in the Supplemental Information. Although many of the measures used to classify individuals as a "user" are valid, this may potentially introduce some noise within our results. On the other hand, this may

also suggest that our present results appear robustly across differing diagnostic criteria for substance use. Second, the co-occurring use of substances warrants attention. Polysubstance use is a common occurrence in the addiction literature that reflects the difficult nature of recruiting participants that have used only one primary drug throughout their lifetime. Provided such, polysubstance using individuals may actually be the most representative sample for substance research. Third, a greater number of male-using participants are included in the primary literature as compared to female-using. This distribution is also reflective in the non-using control groups as they are often matched samples. The addiction literature as a whole need to make a concerted effort in balancing the distribution of females and males within a study to promote inclusivity and improve individualized treatment practices. Fourth, the limited number of prior studies examining GM differences between substance users and non-users in certain drug classes (e.g., cannabis and opiate) may have limited our ability to detect drug-specific meta-analytic effects. Finally, all meta-analyses are susceptible to biases across the literature and limited by the primary studies' designs, and only significant brain reduction peaks reported by those primary studies (i.e., publication bias). However, our results closely replicate the Mackey and colleagues (2019) ENIGMA consortium, mega-analysis findings in a more cost- and time-effective manner.

5. Conclusions

In sum, this study employed emergent coordinate-based meta-analytic techniques to characterize the functional profiles of structurally altered GM regions consistently observed across substances of abuse and utilized data-driven techniques to delineate what the potentially behavioral implications of such brain alterations may be. Through the application of meta-analytic techniques, we identified convergent regions of reduced GM volume across pharmacological classes of drugs in regions critical for motivation, reward processing, and cognition. We subsequently

characterized the functional connectivity of these regions to delineate a larger extended network, representing a core set of regions strongly connected to multiple structurally altered regions. The extended network was found to be composed of three subnetworks that closely correspond to the tripartite network model, where the dynamic interactions between and within these large-scale brain networks has shown to have important implications in stages of the addiction cycle.

Acknowledgements

Primary funding for this project was provided by NIH R01 DA041353; additional support was provided by NSF 1631325, NIH U01 DA041156, NSF CNS 1532061, NIH K01 DA037819, NIH U54 MD012393.

REFERENCES

Alizadehgoradel, J., Nejati, V., Movahed, F. S., Imani, S., Taherifard, M., Mosayebi-Samani, M., . . . Salehinejad, M. A. (2020). Repeated stimulation of the dorsolateral-prefrontal cortex improves executive dysfunctions and craving in drug addiction: A randomized, double-blind, parallel-group study. *Brain Stimulation, 13*(3), 582-593. doi:10.1016/j.brs.2019.12.028

Amft, M., Bzdok, D., Laird, A., Fox, P., Schilbach, L., & Eickhoff, S. (2015). Definition and characterization of an extended social-affective default network. *Brain Structure & Function, 220*(2), 1031-1049. doi:10.1007/s00429-013-0698-0

Andrews-Hanna, J. R., Smallwood, J., & Spreng, R. N. (2014). The default network and self-generated thought: component processes, dynamic control, and clinical relevance. *Year in Cognitive Neuroscience, 1316*, 29-52. doi:10.1111/nyas.12360

Bartley, J. E., Boeving, E. R., Riedel, M. C., Bottenhorn, K. L., Salo, T., Eickhoff, S. B., . . . Laird, A. R. (2018). Meta-analytic evidence for a core problem solving network across multiple representational domains. *Neurosci Biobehav Rev, 92*, 318-337. doi:10.1016/j.neubiorev.2018.06.009

Bechara, A., Damasio, A. R., Damasio, H., & Anderson, S. W. (1994). Insensitivity to Future Consequences Following Damage to Human Prefrontal Cortex. *Cognition, 50*(1-3), 7-15. doi:Doi 10.1016/0010-0277(94)90018-3

Bechara, A., Damasio, H., Tranel, D., & Damasio, A. R. (1997). Deciding advantageously before knowing the advantageous strategy. *Science, 275*(5304), 1293-1295. doi:DOI 10.1126/science.275.5304.1293

Binder, J. R., Frost, J. A., Hammeke, T. A., Bellgowan, P. S. F., Rao, S. M., & Cox, R. W. (1999). Conceptual processing during the conscious resting state: A functional MRI study. *Journal of cognitive neuroscience, 11*(1), 80-93. doi:Doi 10.1162/089892999563265

Boes, A. D. (2021). Lesion network mapping: where do we go from here? *Brain, 144*. doi:ARTN e5 10.1093/brain/awaa350

Boes, A. D., Prasad, S., Liu, H. S., Liu, Q., Pascual-Leone, A., Caviness, V. S., & Fox, M. D. (2015). Network localization of neurological symptoms from focal brain lesions. *Brain, 138*, 3061-3075. doi:10.1093/brain/awv228

Bottenhorn, K. L., Flannery, J. S., Boeving, E. R., Riedel, M. C., Eickhoff, S. B., Sutherland, M. T., & Laird, A. R. (2019). Cooperating yet distinct brain networks engaged during naturalistic paradigms: A meta-analysis of functional MRI results. *Netw Neurosci, 3*(1), 27-48. doi:10.1162/netn_a_00050

Botvinick, M. M., Braver, T. S., Barch, D. M., Carter, C. S., & Cohen, J. D. (2001). Conflict monitoring and cognitive control. *Psychological Review, 108*(3), 624-652. doi:10.1037//0033-295x.108.3.624

Buckley, M. J., Mansouri, F. A., & Tanaka, K. (2009). Dissociable components of rule-guided decision-making and executive control supported by different prefrontal and medial frontal cortical regions. *Neuroscience Research, 65*, S30-S30. doi:10.1016/j.neures.2009.09.1666

Buckner, R. L., Andrews-Hanna, J. R., & Schacter, D. L. (2008). The brain's default network: anatomy, function, and relevance to disease. *Ann N Y Acad Sci, 1124*, 1-38. doi:10.1196/annals.1440.011

Burgess, G. C., Kandala, S., Nolan, D., Laumann, T. O., Power, J. D., Adeyemo, B., . . . Barch, D. M. (2016). Evaluation of Denoising Strategies to Address Motion-Correlated Artifacts in Resting-State Functional Magnetic Resonance Imaging Data from the Human Connectome Project. *Brain Connectivity, 6*(9), 669-680. doi:10.1089/brain.2016.0435

Bush, G., Luu, P., & Posner, M. I. (2000). Cognitive and emotional influences in anterior cingulate cortex. *Trends in Cognitive Sciences, 4*(6), 215-222. doi:Doi 10.1016/S1364-6613(00)01483-2

Camille, N., Tsuchida, A., & Fellows, L. K. (2011). Double Dissociation of Stimulus-Value and Action-Value Learning in Humans with Orbitofrontal or Anterior Cingulate Cortex Damage. *Journal of Neuroscience, 31*(42), 15048-15052. doi:10.1523/Jneurosci.3164-11.2011

Camilleri, J. A., Muller, V. I., Fox, P., Laird, A. R., Hoffstaedter, F., Kalenscher, T., & Eickhoff, S. B. (2018). Definition and characterization of an extended multiple-demand network. *Neuroimage, 165*, 138-147. doi:10.1016/j.neuroimage.2017.10.020

Chang, L. J., Yarkoni, T., Khaw, M. W., & Sanfey, A. G. (2013). Decoding the Role of the Insula in Human Cognition: Functional Parcellation and Large-Scale Reverse Inference. *Cerebral cortex, 23*(3), 739-749. doi:10.1093/cercor/bhs065

Craig, A. D. (2009). How do you feel - now? The anterior insula and human awareness. *Nature reviews neuroscience, 10*(1), 59-70. doi:10.1038/nrn2555

Darby, R. R., Laganiere, S., Pascual-Leone, A., Prasad, S., & Fox, M. D. (2017). Finding the imposter: brain connectivity of lesions causing delusional misidentifications. *Brain, 140*, 497-507. doi:10.1093/brain/aww288

Deen, B., Pitskel, N. B., & Pelphrey, K. A. (2011). Three Systems of Insular Functional Connectivity Identified with Cluster Analysis. *Cerebral cortex, 21*(7), 1498-1506. doi:10.1093/cercor/bhq186

Devinsky, O., Morrell, M. J., & Vogt, B. A. (1995). Contributions of Anterior Cingulate Cortex to Behaviour. *Brain, 118*, 279-306. doi:DOI 10.1093/brain/118.1.279

Eickhoff, S. B., Bzdok, D., Laird, A. R., Kurth, F., & Fox, P. T. (2012). Activation likelihood estimation meta-analysis revisited. *Neuroimage, 59*(3), 2349-2361. doi:10.1016/j.neuroimage.2011.09.017

Eickhoff, S. B., Laird, A. R., Fox, P. M., Lancaster, J. L., & Fox, P. T. (2017). Implementation errors in the GingerALE Software: Description and recommendations. *Hum Brain Mapp, 38*(1), 7-11. doi:10.1002/hbm.23342

Eickhoff, S. B., Laird, A. R., Grefkes, C., Wang, L. E., Zilles, K., & Fox, P. T. . (2009). Coordinate-based ALE meta-analysis of neuroimaging data: a random-effects approach based on empirical estimates of spatial uncertainty. *Human brain mapping, 30*(9), 2907. doi:0.1002/hbm.20718

Eickhoff, S. B., Nichols, T. E., Laird, A. R., Hoffstaedter, F., Amunts, K., Fox, P. T., . . . Eickhoff, C. R. (2016). Behavior, sensitivity, and power of activation likelihood estimation characterized by massive empirical simulation. *Neuroimage, 137*, 70-85. doi:10.1016/j.neuroimage.2016.04.072

Ersche, K. D., Williams, G. B., Robbins, T. W., & Bullmore, E. T. (2013). Meta-analysis of structural brain abnormalities associated with stimulant drug dependence and neuroimaging of addiction vulnerability and resilience. *Curr Opin Neurobiol, 23*(4), 615-624. doi:10.1016/j.conb.2013.02.017

Everitt, B. J., & Robbins, T. W. (2005). Neural systems of reinforcement for drug addiction: from actions to habits to compulsion. *Nat Neurosci, 8*(11), 1481-1489. doi:10.1038/nn1579

Fedota, J. R., & Stein, E. A. (2015). Resting-state functional connectivity and nicotine addiction: prospects for biomarker development. *Ann N Y Acad Sci, 1349*, 64-82. doi:10.1111/nyas.12882

Feinberg, D. A., Moeller, S., Smith, S. M., Auerbach, E., Ramanna, S., Gunther, M., . . . Yacoub, E. (2010). Multiplexed echo planar imaging for sub-second whole brain FMRI and fast diffusion imaging. *PloS one, 5*(12), e15710. doi:10.1371/journal.pone.0015710

Ferguson, M. A., Lim, C., Cooke, D., Darby, R. R., Wu, O., Rost, N. S., . . . Fox, M. D. (2019). A human memory circuit derived from brain lesions causing amnesia. *Nature Communications, 10*. doi:ARTN 3497

10.1038/s41467-019-11353-z

Flannery, J. S., Riedel, M. C., Bottenhorn, K. L., Poudel, R., Salo, T., Hill-Bowen, L. D., . . . Sutherland, M. T. (2020). Meta-analytic clustering dissociates brain activity and behavior profiles across reward processing paradigms. *Cogn Affect Behav Neurosci, 20*(2), 215-235. doi:10.3758/s13415-019-00763-7

Fox, M. D., Snyder, A. Z., Vincent, J. L., Corbetta, M., Van Essen, D. C., & Raichle, M. E. (2005). The human brain is intrinsically organized into dynamic, anticorrelated functional networks. *Proc Natl Acad Sci U S A, 102*(27), 9673-9678. doi:10.1073/pnas.0504136102

Garavan, H., & Stout, J. C. (2005). Neurocognitive insights into substance abuse. *Trends Cogn Sci, 9*(4), 195-201. doi:10.1016/j.tics.2005.02.008

Glasser, M. F., Smith, S. M., Marcus, D. S., Andersson, J. L., Auerbach, E. J., Behrens, T. E., . . . Van Essen, D. C. (2016). The Human Connectome Project's neuroimaging approach. *Nat Neurosci, 19*(9), 1175-1187. doi:10.1038/nn.4361

Goldstein, R. Z., & Volkow, N. D. (2002). Drug addiction and its underlying neurobiological basis: neuroimaging evidence for the involvement of the frontal cortex. *American Journal of Psychiatry, 159*(10), 1642-1652.

Goodkind, M., Eickhoff, S. B., Oathes, D. J., Jiang, Y., Chang, A., Jones-Hagata, L. B., . . . Etkin, A. (2015). Identification of a common neurobiological substrate for mental illness. *JAMA Psychiatry, 72*(4), 305-315. doi:10.1001/jamapsychiatry.2014.2206

Greicius, M. D., Krasnow, B., Reiss, A. L., & Menon, V. (2003). Functional connectivity in the resting brain: a network analysis of the default mode hypothesis. *Proc Natl Acad Sci U S A, 100*(1), 253-258. doi:10.1073/pnas.0135058100

Haber, S. N. (2003). The primate basal ganglia: parallel and integrative networks. *Journal of Chemical Neuroanatomy, 26*(4), 317-330. doi:10.1016/j.jchemneu.2003.10.003

Haber, S. N., Fudge, J. L., & McFarland, N. R. (2000). Striatonigrostriatal pathways in primates form an ascending spiral from the shell to the dorsolateral striatum. *Journal of Neuroscience, 20*(6), 2369-2382. Retrieved from <Go to ISI>://WOS:000085724200035

Hall, M. G., Alhassoon, O. M., Stern, M. J., Wollman, S. C., Kimmel, C. L., Perez-Figueroa, A., & Radua, J. (2015). Gray matter abnormalities in cocaine versus methamphetamine-dependent patients: a neuroimaging meta-analysis. *Am J Drug Alcohol Abuse, 41*(4), 290-299. doi:10.3109/00952990.2015.1044607

Hayden, B. Y., Nair, A. C., McCoy, A. N., & Platt, M. L. (2008). Posterior cingulate cortex mediates outcome-contingent allocation of behavior. *Neuron, 60*(1), 19-25. doi:10.1016/j.neuron.2008.09.012

Hill-Bowen, L. D., Riedel, M. C., Poudel, R., Salo, T., Flannery, J. S., Camilleri, J. A., . . . Sutherland, M. T. (2021). The cue-reactivity paradigm: An ensemble of networks driving attention and cognition when viewing drug and natural reward-related stimuli. *Neurosci Biobehav Rev, 130*, 201-213. doi:10.1016/j.neubiorev.2021.08.010

Hill-Bowen, L. D., Riedel, M.C., Poudel, R., Salo, T., Flannery J.S., Camilleri, J.A., Eickhoff, S.B., Laird, A.R., Sutherland, M.T. (2020). The cue-reactivity paradigm: An ensemble of networks driving attention and cognition when viewing drug-related and natural-reward stimuli. *bioRxiv*, 2020.2002.2026.966549. doi:10.1101/2020.02.26.966549

Hochman, E. Y., Wang, S. Q., Milner, T. E., & Fellows, L. K. (2015). Double dissociation of error inhibition and correction deficits after basal ganglia or dorsomedial frontal damage in humans. *Neuropsychologia, 69*, 130-139. doi:10.1016/j.neuropsychologia.2015.01.023

Honey, C. J., Kotter, R., Breakspear, M., & Sporns, O. (2007). Network structure of cerebral cortex shapes functional connectivity on multiple time scales. *Proc Natl Acad Sci U S A, 104*(24), 10240-10245. doi:10.1073/pnas.0701519104

Hornak, J., O'Doherty, J., Bramham, J., Rolls, E. T., Morris, R. G., Bullock, P. R., & Polkey, C. E. (2004). Reward-related reversal learning after surgical excisions in orbito-frontal or dorsolateral prefrontal cortex in humans. *Journal of cognitive neuroscience, 16*(3), 463-478. doi:Doi 10.1162/089892904322926791

Ibrahim, C., Rubin-Kahana, D. S., Pushparaj, A., Musiol, M., Blumberger, D. M., Daskalakis, Z. J., . . . Le Foll, B. (2019). The Insula: A Brain Stimulation Target for the Treatment of Addiction. *Frontiers in Pharmacology, 10*. doi:ARTN 720
10.3389/fphar.2019.00720

Janes, A. C., Datko, M., Roy, A., Barton, B., Druker, S., Neal, C., . . . Brewer, J. A. (2019). Quitting starts in the brain: a randomized controlled trial of app-based mindfulness shows decreases in neural responses to smoking cues that predict reductions in smoking. *Neuropsychopharmacology, 44*(9), 1631-1638. doi:10.1038/s41386-019-0403-y

Janes, A. C., Farmer, S., Peechatka, A. L., Frederick, B. D., & Lukas, S. E. (2015). Insula-Dorsal Anterior Cingulate Cortex Coupling is Associated with Enhanced Brain Reactivity to Smoking Cues. *Neuropsychopharmacology, 40*(7), 1561-1568. doi:10.1038/npp.2015.9

Janes, A. C., Krantz, N. L., Nickerson, L. D., Frederick, B. B., & Lukas, S. E. (2020). Craving and Cue Reactivity in Nicotine-Dependent Tobacco Smokers Is Associated With Different Insula Networks. *Biological Psychiatry-Cognitive Neuroscience and Neuroimaging, 5*(1), 76-83. doi:10.1016/j.bpsc.2019.09.005

Jarraya, B., Brugieres, P., Tani, N., Hodel, J., Grandjacques, B., Fenelon, G., . . . Palfi, S. (2010). Disruption of cigarette smoking addiction after posterior cingulate damage. *Journal of Neurosurgery, 113*(6), 1219-1221. doi:10.3171/2010.6.Jns10346

Jenkinson, M., Beckmann, C. F., Behrens, T. E., Woolrich, M. W., & Smith, S. M. (2012). Fsl. *Neuroimage, 62*(2), 782-790. doi:10.1016/j.neuroimage.2011.09.015

Joutsa, J., Shih, L. C., & Fox, M. D. (2019). Mapping holmes tremor circuit using the human brain connectome. *Annals of Neurology, 86*(6), 812-820. doi:10.1002/ana.25618

Kennerley, S. W., Walton, M. E., Behrens, T. E. J., Buckley, M. J., & Rushworth, M. F. S. (2006). Optimal decision making and the anterior cingulate cortex. *Nature neuroscience, 9*(7), 940-947. doi:10.1038/nn1724

Kim, N. Y., Hsu, J., Talmasov, D., Joutsa, J., Soussand, L., Wu, O., . . . Fox, M. D. (2021). Lesions causing hallucinations localize to one common brain network. *Molecular Psychiatry, 26*(4), 1299-1309. doi:10.1038/s41380-019-0565-3

Klaming, R., Harle, K. M., Infante, M. A., Bomyea, J., Kim, C., & Spadoni, A. D. (2019). Shared gray matter reductions across alcohol use disorder and posttraumatic stress disorder in the anterior cingulate cortex: A dual meta-analysis. *Neurobiol Stress, 10*, 100132. doi:10.1016/j.ynstr.2018.09.009

Kolling, N., Wittmann, M. K., Behrens, T. E. J., Boorman, E. D., Mars, R. B., & Rushworth, M. F. S. (2016). Value, search, persistence and model updating in anterior cingulate cortex. *Nature neuroscience, 19*(10), 1280-1285. doi:10.1038/nn.4382

Koob, G. F., & Volkow, N. D. (2010). Neurocircuitry of addiction. *Neuropsychopharmacology, 35*(1), 217-238. doi:10.1038/npp.2009.110

Koob, G. F., & Volkow, N. D. (2016). Neurobiology of addiction: a neurocircuitry analysis. *Lancet Psychiatry, 3*(8), 760-773. doi:10.1016/S2215-0366(16)00104-8

Koski, L., & Paus, T. (2000). Functional connectivity of the anterior cingulate cortex within the human frontal lobe: a brain-mapping meta-analysis. *Experimental Brain Research, 133*(1), 55-65. doi:DOI 10.1007/s002210000400

Kumral, E., Erdogan, C. E., Bayam, F. E., & Arslan, H. (2019). Cingulate infarction: A neuropsychological and neuroimaging study. *Journal of the Neurological Sciences, 402*, 1-6. doi:10.1016/j.jns.2019.04.033

Laird, A. R., Eickhoff, S. B., Li, K., Robin, D. A., Glahn, D. C., & Fox, P. T. (2009). Investigating the functional heterogeneity of the default mode network using coordinate-based meta-analytic modeling. *J Neurosci, 29*(46), 14496-14505. doi:10.1523/JNEUROSCI.4004-09.2009

Laird, A. R., Fox, P. M., Price, C. J., Glahn, D. C., Uecker, A. M., Lancaster, J. L., . . . Fox, P. T. (2005). ALE meta-analysis: controlling the false discovery rate and performing statistical contrasts. *Hum Brain Mapp, 25*(1), 155-164. doi:10.1002/hbm.20136

Lancaster, J. L., Tordesillas-Gutierrez, D., Martinez, M., Salinas, F., Evans, A., Zilles, K., . . . Fox, P. T. (2007). Bias between MNI and Talairach coordinates analyzed using the ICBM-152 brain template. *Hum Brain Mapp, 28*(11), 1194-1205. doi:10.1002/hbm.20345

Leech, R., Kamourieh, S., Beckmann, C. F., & Sharp, D. J. (2011). Fractionating the Default Mode Network: Distinct Contributions of the Ventral and Dorsal Posterior Cingulate Cortex to Cognitive Control. *Journal of Neuroscience, 31*(9), 3217-3224. doi:10.1523/Jneurosci.5626-10.2011

Mackey, S., Allgaier, N., Chaarani, B., Spechler, P., Orr, C., Bunn, J., . . . Group, E. A. W. (2019). Mega-Analysis of Gray Matter Volume in Substance Dependence: General and Substance-Specific Regional Effects. *Am J Psychiatry, 176*(2), 119-128. doi:10.1176/appi.ajp.2018.17040415

Mansouri, F. A., Tanaka, K., & Buckley, M. J. (2009). Conflict-induced behavioural adjustment: a clue to the executive functions of the prefrontal cortex (vol 10, pg 141, 2009). *Nature reviews neuroscience, 10*(3). doi:10.1038/nrn2596

Menon, V. (2011). Large-scale brain networks and psychopathology: a unifying triple network model. *Trends Cogn Sci, 15*(10), 483-506. doi:10.1016/j.tics.2011.08.003

Menon, V., & Uddin, L. Q. (2010). Saliency, switching, attention and control: a network model of insula function. *Brain Structure & Function, 214*(5-6), 655-667. doi:10.1007/s00429-010-0262-0

Naqvi, N. H., & Bechara, A. (2009). The hidden island of addiction: the insula. *Trends Neurosci, 32*(1), 56-67. doi:10.1016/j.tins.2008.09.009

Naqvi, N. H., Rudrauf, D., Damasio, H., & Bechara, A. (2007). Damage to the insula disrupts addiction to cigarette smoking. *Science, 315*(5811), 531-534. doi:10.1126/science.1135926

NIDA. (2017). Trends & Statistics. Retrieved from https://www.drugabuse.gov/related-topics/trends-statistics

NIDA. (2018). Principles of Drug Addiction Treatment: A Research-Based Guide Third. Retrieved from https://www.drugabuse.gov/publications/principles-drug-addiction-treatment-research-based-guide-third-edition

O'Doherty, J., Kringelbach, M. L., Rolls, E. T., Hornak, J., & Andrews, C. (2001). Abstract reward and punishment representations in the human orbitofrontal cortex. *Nature neuroscience, 4*(1), 95-102. Retrieved from <Go to ISI>://WOS:000167178000020

Padmanabhan, J. L., Cooke, D., Joutsa, J., Siddiqi, S. H., Ferguson, M., Darby, R. R., . . . Fox, M. D. (2019). A Human Depression Circuit Derived From Focal Brain Lesions. *Biological psychiatry, 86*(10), 749-758. doi:10.1016/j.biopsych.2019.07.023

Pan, P., Shi, H., Zhong, J., Xiao, P., Shen, Y., Wu, L., . . . He, G. (2012). Chronic smoking and brain gray matter changes: evidence from meta-analysis of voxel-based morphometry studies. *Neurological Sciences, 34*(6), 813-817. doi:10.1007/s10072-012-1256-x

Pauli, W. M., O'Reilly, R. C., Yarkoni, T., & Wager, T. D. (2016). Regional specialization within the human striatum for diverse psychological functions. *Proceedings of the National Academy of Sciences of the United States of America, 113*(7), 1907-1912. doi:10.1073/pnas.1507610113

Pearson, J. M., Heilbronner, S. R., Barack, D. L., Hayden, B. Y., & Platt, M. L. (2011). Posterior cingulate cortex: adapting behavior to a changing world. *Trends Cogn Sci, 15*(4), 143-151. doi:10.1016/j.tics.2011.02.002

Petrides, M. (2005). Lateral prefrontal cortex: architectonic and functional organization. *Philosophical Transactions of the Royal Society B-Biological Sciences, 360*(1456), 781-795. doi:10.1098/rstb.2005.1631

Philippi, C. L., Bruss, J., Boes, A. D., Albazron, F. M., Streese, C. D., Ciaramelli, E., . . . Tranel, D. (2021). Lesion network mapping demonstrates that mind-wandering is associated with the default mode network. *Journal of neuroscience research, 99*(1), 361-373. doi:10.1002/jnr.24648

Poudel, R., Riedel, M. C., Salo, T., Flannery, J. S., Hill-Bowen, L. D., Eickhoff, S. B., . . . Sutherland, M. T. (2020). Common and distinct brain activity associated with risky and ambiguous decision-making. *Drug and alcohol dependence, 209*. doi:ARTN 107884
10.1016/j.drugalcdep.2020.107884

Qin, P., & Northoff, G. (2011). How is our self related to midline regions and the default-mode network? *Neuroimage, 57*(3), 1221-1233. doi:10.1016/j.neuroimage.2011.05.028

Rangel, A., Camerer, C., & Montague, P. R. (2008). A framework for studying the neurobiology of value-based decision making. *Nature reviews neuroscience, 9*(7), 545-556. doi:10.1038/nrn2357

Ridderinkhof, K. R., van den Wildenberg, W. P. M., Segalowitz, S. J., & Carter, C. S. (2004). Neurocognitive mechanisms of cognitive control: The role of prefrontal cortex in action selection,

response inhibition, performance monitoring, and reward-based learning. *Brain and cognition, 56*(2), 129-140. doi:10.1016/j.bandc.2004.09.016

Rushworth, M. F. S., Walton, M. E., Kennerley, S. W., & Bannerman, D. M. (2004). Action sets and decisions in the medial frontal cortex. *Trends in Cognitive Sciences, 8*(9), 410-417. doi:10.1016/j.tics.2004.07.009

Salimi-Khorshidi, G., Douaud, G., Beckmann, C. F., Glasser, M. F., Griffanti, L., & Smith, S. M. (2014). Automatic denoising of functional MRI data: combining independent component analysis and hierarchical fusion of classifiers. *Neuroimage, 90*, 449-468. doi:10.1016/j.neuroimage.2013.11.046

Salimi-Khorshidi, G., Smith, S. M., Keltner, J. R., Wager, T. D., & Nichols, T. E. (2009). Meta-analysis of neuroimaging data: a comparison of image-based and coordinate-based pooling of studies. *Neuroimage, 45*(3), 810-823. doi:10.1016/j.neuroimage.2008.12.039

Salling, M. C., & Martinez, D. (2016). Brain Stimulation in Addiction. *Neuropsychopharmacology, 41*(12), 2798-2809. doi:10.1038/npp.2016.80

Schneider, B., & Koenigs, M. (2017). Human lesion studies of ventromedial prefrontal cortex. *Neuropsychologia, 107*, 84-93. doi:10.1016/j.neuropsychologia.2017.09.035

Seeley, W. W., Menon, V., Schatzberg, A. F., Keller, J., Glover, G. H., Kenna, H., . . . Greicius, M. D. (2007). Dissociable intrinsic connectivity networks for salience processing and executive control. *J Neurosci, 27*(9), 2349-2356. doi:10.1523/JNEUROSCI.5587-06.2007

Seo, D. J., Lacadie, C. M., Tuit, K., Hong, K. I., Constable, R. T., & Sinha, R. (2013). Disrupted Ventromedial Prefrontal Function, Alcohol Craving, and Subsequent Relapse Risk. *JAMA Psychiatry, 70*(7), 727-739. doi:10.1001/jamapsychiatry.2013.762

Sestieri, C., Corbetta, M., Romani, G. L., & Shulman, G. L. (2011). Episodic Memory Retrieval, Parietal Cortex, and the Default Mode Network: Functional and Topographic Analyses. *Journal of Neuroscience, 31*(12), 4407-4420. doi:10.1523/Jneurosci.3335-10.2011

Sha, Z., Wager, T. D., Mechelli, A., & He, Y. (2019). Common Dysfunction of Large-Scale Neurocognitive Networks Across Psychiatric Disorders. *Biol Psychiatry, 85*(5), 379-388. doi:10.1016/j.biopsych.2018.11.011

Shenhav, A., Cohen, J. D., & Botvinick, M. M. (2016). Dorsal anterior cingulate cortex and the value of control. *Nature neuroscience, 19*(10), 1286-1291. doi:DOI 10.1038/nn.4384

Shima, K., & Tanji, J. (1998). Role for cingulate motor area cells in voluntary movement selection based on reward. *Science, 282*(5392), 1335-1338. doi:DOI 10.1126/science.282.5392.1335

Smith, S. M., Beckmann, C. F., Andersson, J., Auerbach, E. J., Bijsterbosch, J., Douaud, G., . . . Consortium, W. U.-M. H. (2013). Resting-state fMRI in the Human Connectome Project. *Neuroimage, 80*, 144-168. doi:10.1016/j.neuroimage.2013.05.039

Spreng, R. N., Mar, R. A., & Kim, A. S. N. (2009). The Common Neural Basis of Autobiographical Memory, Prospection, Navigation, Theory of Mind, and the Default Mode: A Quantitative Meta-analysis. *Journal of cognitive neuroscience, 21*(3), 489-510. doi:DOI 10.1162/jocn.2008.21029

Sridharan, D., Levitin, D. J., & Menon, V. (2008a). A critical role for the right fronto-insular cortex in switching between central-executive and default-mode networks. *Proceedings of the National Academy of Sciences of the United States of America, 105*(34), 12569-12574. doi:10.1073/pnas.0800005105

Sridharan, D., Levitin, D. J., & Menon, V. (2008b). A critical role for the right fronto-insular cortex in switching between central-executive and default-mode networks. *Proceedings of the National Academy of Sciences, 105*(34), 12569-12574. doi:10.1073/pnas.0800005105

Su, H., Zhong, N., Gan, H., Wang, J. J., Han, H., Chen, T. Z., . . . Zhao, M. (2017). High frequency repetitive transcranial magnetic stimulation of the left dorsolateral prefrontal cortex for methamphetamine use disorders: A randomised clinical trial. *Drug and alcohol dependence, 175*, 84-91. doi:10.1016/j.drugalcdep.2017.01.037

Sutherland, M. T., McHugh, M. J., Pariyadath, V., & Stein, E. A. (2012a). Resting state functional connectivity in addiction: Lessons learned and a road ahead. *Neuroimage, 62*(4), 2281-2295. doi:10.1016/j.neuroimage.2012.01.117

Sutherland, M. T., McHugh, M. J., Pariyadath, V., & Stein, E. A. (2012b). Resting state functional connectivity in addiction: Lessons learned and a road ahead. *Neuroimage, 62*(4), 2281-2295. doi:10.1016/j.neuroimage.2012.01.117

Sutherland, M. T., Ray, K. L., Riedel, M. C., Yanes, J. A., Stein, E. A., & Laird, A. R. (2015). Neurobiological Impact of Nicotinic Acetylcholine Receptor Agonists: An Activation Likelihood Estimation Meta-Analysis of Pharmacologic Neuroimaging Studies. *Biological psychiatry, 78*(10), 711-720. doi:10.1016/j.biopsych.2014.12.021

Sutherland, M. T., Riedel, M. C., Flannery, J. S., Yanes, J. A., Fox, P. T., Stein, E. A., & Laird, A. R. (2016). Chronic cigarette smoking is linked with structural alterations in brain regions showing acute nicotinic drug-induced functional modulations. *Behav Brain Funct, 12*(1), 16. doi:10.1186/s12993-016-0100-5

Sutherland, M. T., & Stein, E. A. (2018). Functional Neurocircuits and Neuroimaging Biomarkers of Tobacco Use Disorder. *Trends in Molecular Medicine, 24*(2), 129-143. doi:10.1016/j.molmed.2017.12.002

Taylor, K. S., Seminowicz, D. A., & Davis, K. D. (2009). Two Systems of Resting State Connectivity Between the Insula and Cingulate Cortex. *Human brain mapping, 30*(9), 2731-2745. doi:10.1002/hbm.20705

Turkeltaub, P. E., Eden, G. F., Jones, K. M., & Zeffiro, T. A. (2002). Meta-analysis of the functional neuroanatomy of single-word reading: method and validation. *Neuroimage, 16*(3 Pt 1), 765-780. doi:10.1006/nimg.2002.1131

Turkeltaub, P. E., Eickhoff, S. B., Laird, A. R., Fox, M., Wiener, M., & Fox, P. (2012). Minimizing within-experiment and within-group effects in Activation Likelihood Estimation meta-analyses. *Hum Brain Mapp, 33*(1), 1-13. doi:10.1002/hbm.21186

Uddin, L. Q. (2015). Salience processing and insular cortical function and dysfunction. *Nature reviews neuroscience, 16*(1), 55-61. doi:10.1038/nrn3857

Ugurbil, K., Xu, J., Auerbach, E. J., Moeller, S., Vu, A. T., Duarte-Carvajalino, J. M., . . . Consortium, W. U.-M. H. (2013). Pushing spatial and temporal resolution for functional and diffusion MRI in the Human Connectome Project. *Neuroimage, 80*, 80-104. doi:10.1016/j.neuroimage.2013.05.012

Van Essen, D. C., Smith, S. M., Barch, D. M., Behrens, T. E., Yacoub, E., Ugurbil, K., & Consortium, W. U.-M. H. (2013). The WU-Minn Human Connectome Project: an overview. *Neuroimage, 80*, 62-79. doi:10.1016/j.neuroimage.2013.05.041

Van Essen, D. C., Ugurbil, K., Auerbach, E., Barch, D., Behrens, T. E., Bucholz, R., . . . Consortium, W. U.-M. H. (2012). The Human Connectome Project: a data acquisition perspective. *Neuroimage, 62*(4), 2222-2231. doi:10.1016/j.neuroimage.2012.02.018

Verdejo-Garcia, A., Lawrence, A. J., & Clark, L. (2008). Impulsivity as a vulnerability marker for substance-use disorders: review of findings from high-risk research, problem gamblers and genetic association studies. *Neurosci Biobehav Rev, 32*(4), 777-810. doi:10.1016/j.neubiorev.2007.11.003

Volkow, N. D., Michaelides, M., & Baler, R. (2019). The Neuroscience of Drug Reward and Addiction. *Physiological Reviews, 99*(4), 2115-2140. doi:10.1152/physrev.00014.2018

Weiland, B. J., Sabbineni, A., Calhoun, V. D., Welsh, R. C., & Hutchison, K. E. (2015). Reduced Executive and Default Network Functional Connectivity in Cigarette Smokers. *Human brain mapping, 36*(3), 872-882. doi:10.1002/hbm.22672

Wollman, S. C., Alhassoon, O. M., Hall, M. G., Stern, M. J., Connors, E. J., Kimmel, C. L., . . . Radua, J. (2016). Gray matter abnormalities in opioid-dependent patients: A neuroimaging meta-analysis. *The American Journal of Drug and Alcohol Abuse, 43*(5), 505-517. doi:10.1080/00952990.2016.1245312

Woo, C. W., Krishnan, A., & Wager, T. D. (2014). Cluster-extent based thresholding in fMRI analyses: pitfalls and recommendations. *Neuroimage, 91*, 412-419. doi:10.1016/j.neuroimage.2013.12.058

Woolrich, M. W., Jbabdi, S., Patenaude, B., Chappell, M., Makni, S., Behrens, T., . . . Smith, S. M. (2009). Bayesian analysis of neuroimaging data in FSL. *Neuroimage, 45*(1 Suppl), S173-186. doi:10.1016/j.neuroimage.2008.10.055

Worsley, K. J. (2001). 14 Statistical analysis of activation images. In *Functional MRI: An introduction to methods* (pp. 251).

Xiao, P., Dai, Z., Zhong, J., Zhu, Y., Shi, H., & Pan, P. (2015). Regional gray matter deficits in alcohol dependence: A meta-analysis of voxel-based morphometry studies. *Drug Alcohol Depend, 153*, 22-28. doi:10.1016/j.drugalcdep.2015.05.030

Yang, X., Tian, F., Zhang, H., Zeng, J., Chen, T., Wang, S., . . . Gong, Q. (2016). Cortical and subcortical gray matter shrinkage in alcohol-use disorders: a voxel-based meta-analysis. *Neurosci Biobehav Rev, 66*, 92-103. doi:10.1016/j.neubiorev.2016.03.034

Yarkoni, T., Poldrack, R. A., Nichols, T. E., Van Essen, D. C., & Wager, T. D. (2011). Large-scale automated synthesis of human functional neuroimaging data. *Nat Methods, 8*(8), 665-670. doi:10.1038/nmeth.1635

Zaborszky, L., Alheid, G. F., Beinfeld, M. C., Eiden, L. E., Heimer, L., & Palkovits, M. (1985). Cholecystokinin Innervation of the Ventral Striatum - a Morphological and Radioimmunological Study. *Neuroscience, 14*(2), 427-+. doi:Doi 10.1016/0306-4522(85)90302-1

Zahm, D. S., & Brog, J. S. (1992). On the Significance of Subterritories in the Accumbens Part of the Rat Ventral Striatum. *Neuroscience, 50*(4), 751-767. doi:Doi 10.1016/0306-4522(92)90202-D

Zhang, R., & Volkow, N. D. (2019). Brain default-mode network dysfunction in addiction. *Neuroimage, 200*, 313-331. doi:10.1016/j.neuroimage.2019.06.036

Zhong, J., Shi, H., Shen, Y., Dai, Z., Zhu, Y., Ma, H., & Sheng, L. (2016). Voxelwise meta-analysis of gray matter anomalies in chronic cigarette smokers. *Behav Brain Res, 311*, 39-45. doi:10.1016/j.bbr.2016.05.016

Figure Captions

PLEASE PRINT THESE FIGURES IN COLOR

Figure 1. Convergent GM reductions across and within drug classes. A) ALE meta-analytic results across all substances identified the left superior frontal, right ACC, bilateral medial frontal, and left insula as convergent regions of reduced GM volume. **B)** ALE results including only alcohol studies identified the bilateral cingulate, left inferior frontal, and left postcentral gyrus as convergent regions of reduced GM. **C)** Meta-analytic results including only nicotine studies identified the left PCC as a region consistently demonstrating reduced GM. **D)** Contrast analyses between alcohol studies and nicotine studies identified the left inferior frontal gyrus and bilateral cingulate gyrus as regions demonstrating reduced GM volume for alcohol as compared to nicotine. No clusters were significantly identified for nicotine – alcohol ($p_{cluster\text{-}level}<0.05$, $p_{voxel\text{-}level}<0.005$).

Figure 2. Functional connections of structurally altered GM regions and associated task-based and task-free subnetworks. A) Regions identified as being functionally connected to those displaying drug-related structural alterations include the right ACC, bilateral PCC, left inferior frontal, right insula, right superior temporal, and left putamen. Color bar values represent the number of overlapping binary consensus maps. **B)** Hierarchical clustering of each region's MACM map (task-based) resulted in three distinct cliques (red, green, and blue). Color bar values represent ALE scores. **C)** Similarly, hierarchical clustering of each region's rsFC map (task-free) resulted in three cliques, with a few notable distinctions from MACM results. ROI 1 (right ACC) clustered with left putamen and left inferior frontal during task-free functional connectivity, as compared to right superior temporal and bilateral PCC during task-based connectivity. Additionally, ROI 2, a second right ACC region, clustered with right insula, right ACC, and left inferior frontal during task-free functional connectivity, as compared to left putamen and left inferior frontal (ROI 5) during task-based connectivity. Vertical axes of dendrograms represent the dissimilarity between clusters based on Ward's minimum variance algorithm.

Figure 3. Characterization of mental operations putatively linked with each task-based subnetwork via Neurosynth functional decoding. A) Visual representation of regions comprising the extended network with colors corresponding to each region's task-based clique grouping. **B)** The size of each shape (i.e., circle, octagon) corresponds to the term ranking from the Neurosynth output, where larger shapes represent terms with greater correlation coefficients and smaller shapes represent terms with lower correlation coefficients. Clique 1 (red) includes functional terms primarily associated with default mode processes, such as *retrieval*, *engaged*, and *mentalizing*, and anatomical terms *medial prefrontal*, *posterior cingulate*, and *prefrontal*. Clique 2 (green) includes functional terms primarily linked with salience attribution, such as *reward*, *incentive*, and *monetary*, and anatomical terms *anterior insula*, *anterior cingulate*, and *striatum*. Finally, Clique 3 (blue) includes functional terms primarily associated with executive functions, such as *task*, *demands*, and *working memory*, and anatomical terms *anterior insula*, *inferior frontal*, and *pre-sma*. A complete list of the top 10 functional and anatomical Neurosynth terms with corresponding term rankings is located in the Supplemental Information.

Tables

Table 1. ALE meta-analytic results of convergent gray matter reductions.

Cluster	Region	Volume	BA	Side	X	Y	Z
A) All Substances							
1	superior frontal gyrus	3504	9	L	-6	56	32
	cingulate gyrus		32	R	4	32	26
	medial frontal gyrus			L	-8	46	20
	anterior cingulate			R	6	44	12
2	medial frontal gyrus	2016		R	8	48	0
3	insula	2040		L	-46	-8	-8
	insula		13	L	-40	8	-8
B) Alcohol							
1	cingulate gyrus	3984	32		0	22	34
2	inferior frontal gyrus	2160	9	L	-50	10	24
3	postcentral gyrus	1832	3	L	-44	-16	48
C) Nicotine							
1	posterior cingulate	1472	30	L	-4	-52	6
	posterior cingulate		30	L	-16	-58	14
D) Alcohol - Nicotine							
1	inferior frontal gyrus	624		L	-52	8	28
2	cingulate gyrus	480			0	28	32

Note. Lettering corresponds to **Figure 1: A, B, C, and D** respectively. Cluster coordinates are based on voxel peak maximum with identified local maxima with each cluster listed below. All cluster coordinates (X, Y, Z) are reported in MNI space. Volume is mm^3.

Table 2. Identified regions comprising the extended network.

Cluster	Region	BA	Side	X	Y	Z
1	anterior cingulate	32	R	2	46	-2
2	anterior cingulate	24	R	2	32	20
3	cingulate gyrus	32	R	2	24	34
4	posterior cingulate	23		0	-52	18
5	inferior frontal gyrus	47	L	-32	18	-14
6	inferior frontal gyrus	45	L	-50	18	0
7	insula	13	R	38	16	-10
8	superior temporal gyrus	39	R	54	-58	24
9	putamen		L	-10	8	-8

Note. Cluster coordinates are based on identified regions of overlap between binary consensus maps of structurally altered gray matter regions across all substances. All cluster coordinates (X, Y, Z) are reported in MNI space.

Figure 1

Click here to access/download;Figure;Figure1_in_TIFF_format.tiff

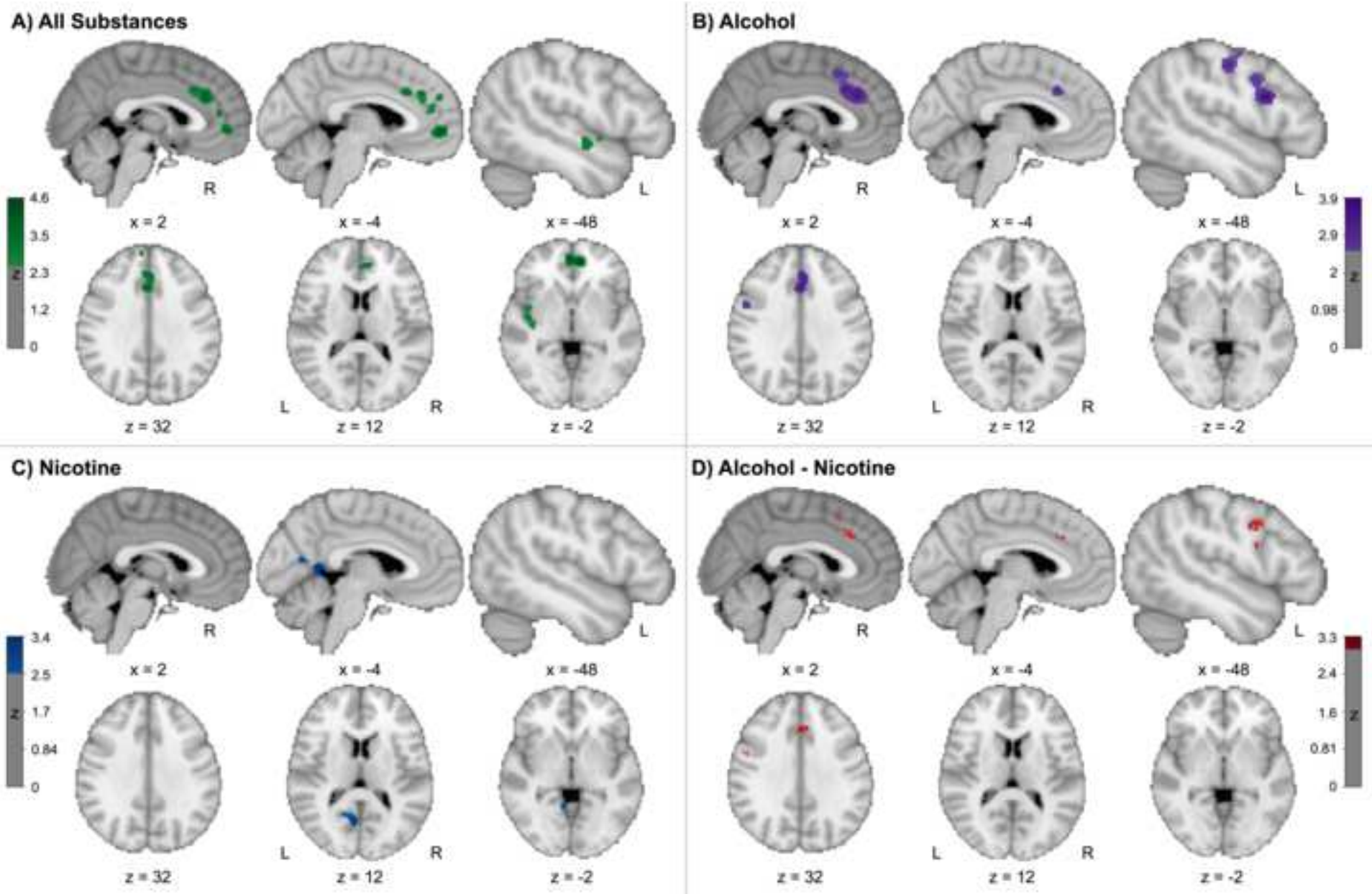

Figure 2

Click here to access/download;Figure;Figure2_in_TIFF_format.tiff

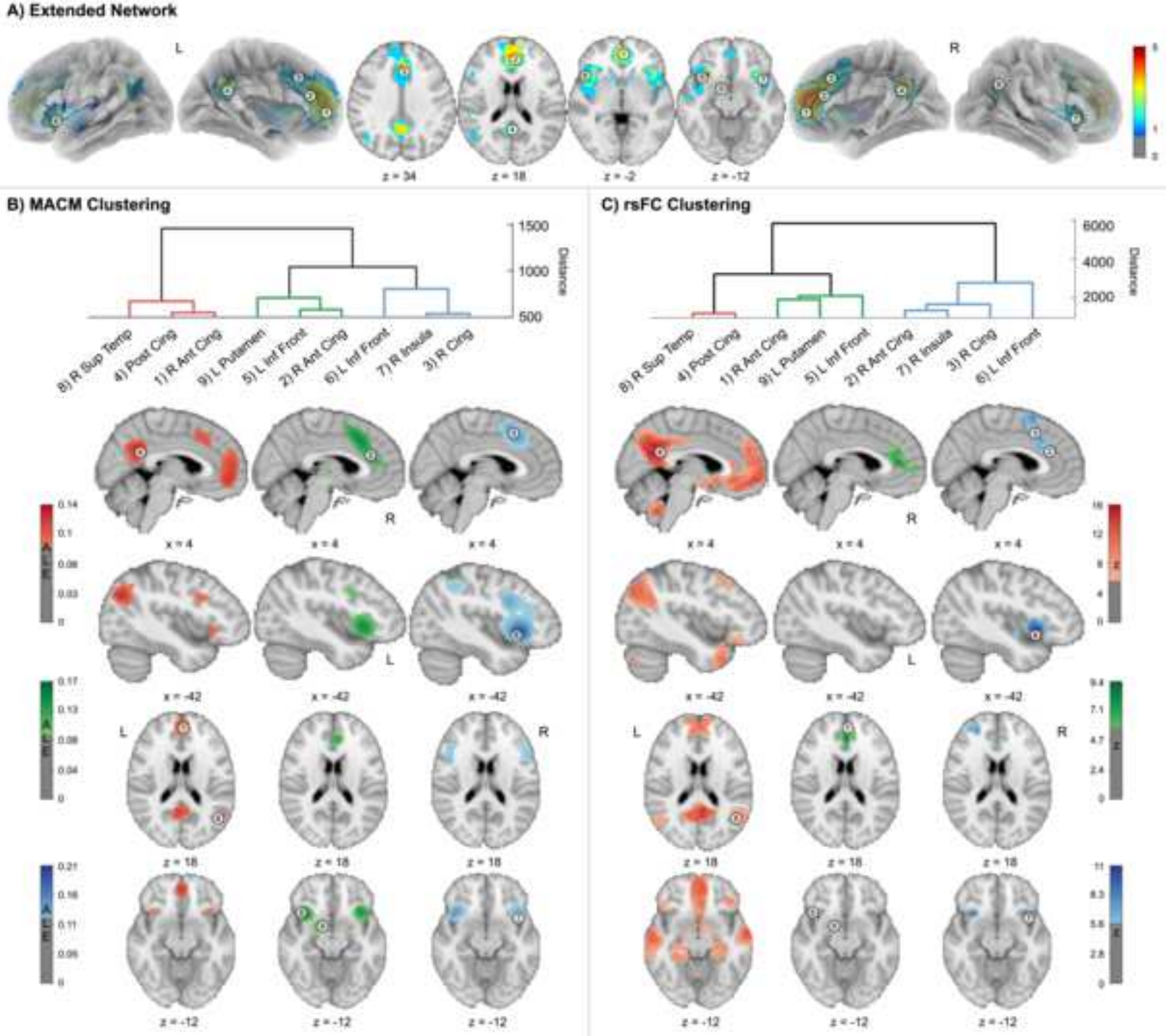

Figure 3

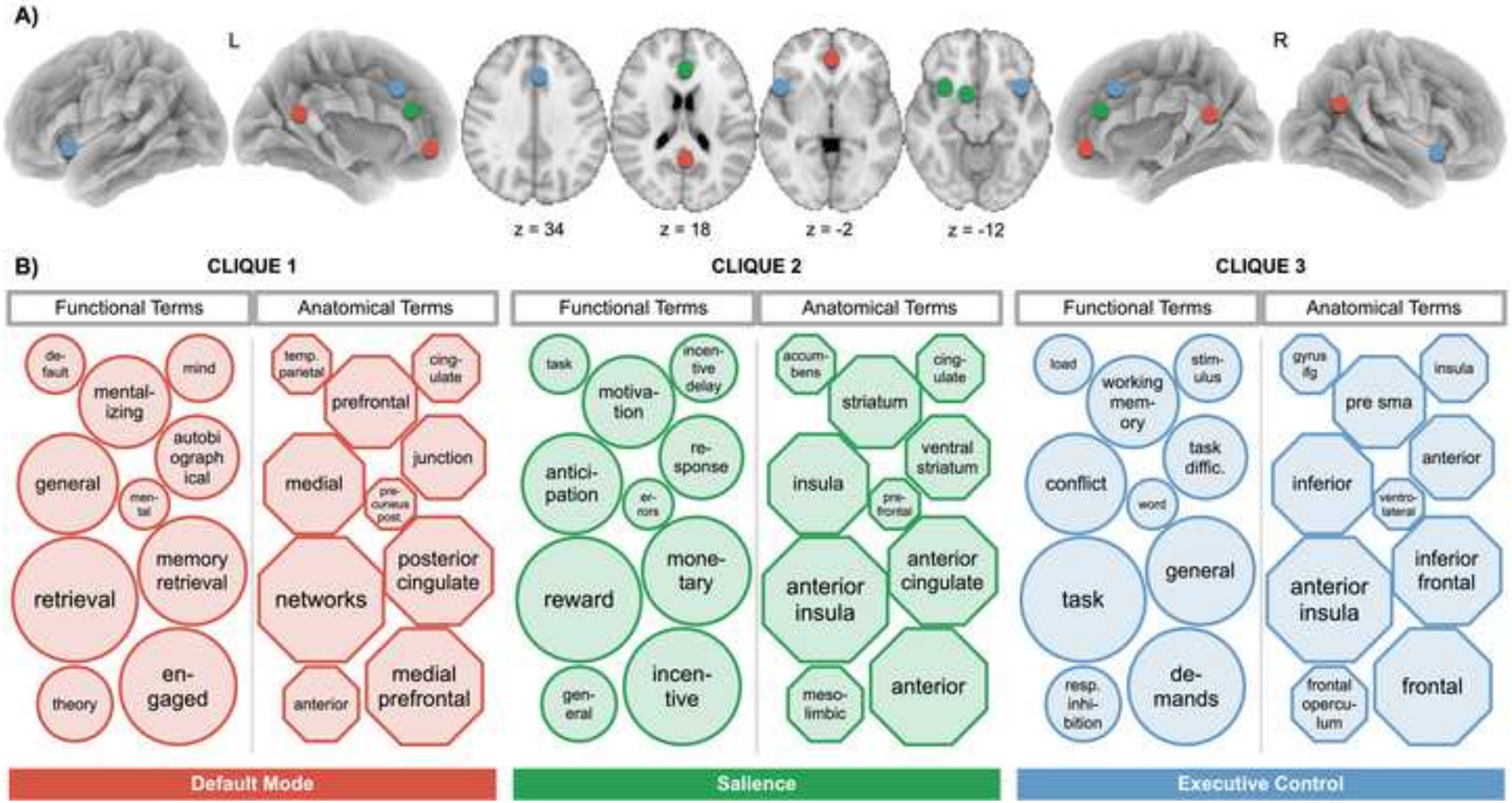

Contributors

Study concept and design: LDH, MCR, MTS. *Acquisition, analysis, or interpretation of data:* All authors. *Drafting of the manuscript:* LDH, MCR, MTS. *Critical revision of the manuscript for important intellectual content:* All authors. *Statistical analysis and meta-analytic tool development:* LDH, MCR, TS, ARL. *Obtained funding:* MTS, ARL. *Administrative, technical, or material support:* MTS, ARL, MCR, TS. *Study supervision:* MTS. *Data:* All data required to evaluate the conclusions in the current article are presented in the paper and/or Supplemental Materials. MTS had full access to all the data in the study and takes responsibility for the integrity of the data and accuracy of data analysis. All authors have read and approved the final manuscript.

Conflict of interest statement

Declaration of interests

☒ The authors declare that they have no known competing financial interests or personal relationships that could have appeared to influence the work reported in this paper.

☐The authors declare the following financial interests/personal relationships which may be considered as potential competing interests: